Dynamic modeling and plantwide control of a production process for biodiesel and glycerol

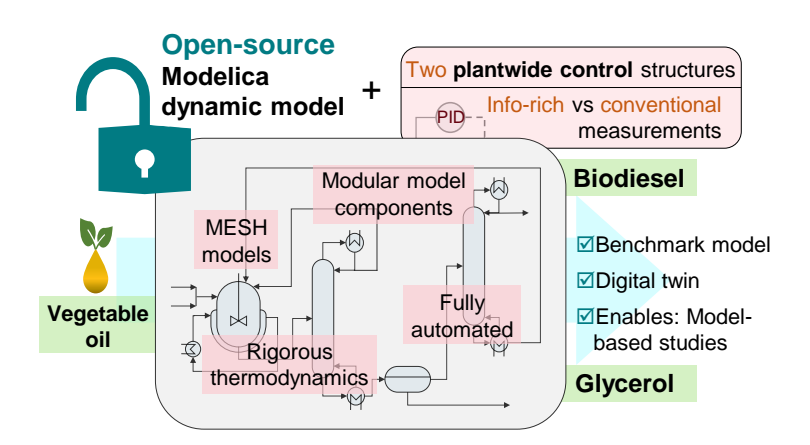
Mohammad El Wajeh¹, Adel Mhamdi¹, and Alexander Mitsos^{2,1,3,*}

¹Process Systems Engineering (AVT.SVT), RWTH Aachen University, 52074 Aachen, Germany ²JARA-CSD, 52056 Aachen, Germany

Keywords — Dynamic modeling, Plantwide control, Biodiesel production, First-principle models, Modelica

Abstract

Biodiesel production comprises several interconnected process steps with complex dynamic behavior. Dynamic plant modeling and simulation enhance process understanding and enable model-based control. We present a modular and rigorous dynamic model for biodiesel and glycerol production by alkali-catalyzed oil transesterification. We share the implemented model in Modelica open-source. Moreover, we implement two plantwide control (PWC) structures, where we assume the availability of information-rich measurements in the first and only conventional measurements in the second. To study the process dynamic behavior, we investigate several disturbance scenarios, demonstrating the importance of the plantwide perspective. The PWC structure based on an information-rich configuration shows satisfactory control performance, whereas the other fails to always satisfy product quality requirements, underlining the importance of developing dynamic models for advanced control and estimation techniques. Moreover, the model can be used as a digital twin for industrial plants as well as for model-based control and estimation applications.



Graphical abstract.

³Energy Systems Engineering (IEK-10), Forschungszentrum Jülich, 52425 Jülich, Germany *Corresponding author: amitsos@alum.mit.edu

1. Introduction

Biomass-based energy has gained importance in recent years. Specifically, biodiesel attracted the attention of both industry and academia in the last decades.^{1,2} It has similar physico-chemical properties to that of petroleum-based diesel.^{1,3} It is biodegradable,⁴ and has low aromatics and sulfur contents.⁵ Biodiesel production processes can use flexible feedstocks.⁶ Biodiesel can be produced from a variety of vegetable oils,⁷ as well as from algae oil or waste cooking oil.⁸

Different catalytic and noncatalytic processes are employed for biodiesel production.^{6,9} Among the noncatalytic supercritical, acid/alkali catalytic heterogeneous and homogeneous transesterification processes, the homogeneous alkali-catalyzed transesterification process is mostly found in practice and has been well considered in the literature.^{3,10–13} It replaces glycerol from oil triglycerides with radicals from the alcohol used for the conversion process in presence of an alkali catalyst. The produced monoesters, known as fatty acid methyl esters (FAMEs), are the biodiesel product.^{14,15} However, the industrial production of biodiesel still faces technical and economic challenges. The final product has to comply with stringent quality standards, while its purification relies on energy-intensive units (distillation), and the raw material may exhibit high variability.⁶ This motivates the development of techniques to improve the economic and operational performance of its production processes while complying with the demanding quality standards.

Biodiesel production involves interconnected unit operations and recycle streams leading to complex process dynamics. Their modeling and simulation improve the understanding of the plant's dynamics and enable economic improvements in its design and operation.

Biodiesel production processes have been considered extensively in the literature from different perspectives. For instance, Mandari and Devaria (2022)¹⁶ reviewed biodiesel production processes using different catalysts, their prospects, and their challenges. Mohiddin et al. (2021)¹⁷ presented a review of the recent advancement and classification of the feedstock and catalyst for biodiesel production. Salvi and Panwar (2012), 18 and Santori et al. (2012)¹⁹ reviewed biodiesel production technologies and resources. Enweremadu and Mbarawa (2009)²⁰ studied the technical aspects of production and quality analysis of biodiesel from used cooking oil. Other studies focused on the techno-economic analysis of different transesterification methods. 3,10,21-25 Lee et al. $(2011)^{26}$ addressed the economic analysis of biodiesel production processes using fresh and waste vegetable oil and supercritical methanol. Zavarukhin et al. (2010)²⁷ focused on the plant design and economics of a biodiesel production and refining process using rapeseed oil. West et al. (2008)²² studied four biodiesel production processes and their economic assessment with different levels of complexity. Other studies focused on the transesterification process only and its kinetic modeling. Noureddini and Zhu (1997)²⁸ modeled the kinetics of the soybean oil transesterification with methanol. Sharma et al. (2011)²⁹ studied the development of heterogeneous catalysts for transesterification reaction processes, and the development of their kinetics was investigated in. 12,30,31 Moreover, other process concepts for biodiesel production have been suggested. Wali et al. (2012)³² developed a novel continuous microwave reactor for the conversion of waste oil and fats into biodiesel, and studied its temperature control. Also, biodiesel production with reactive absorption technology has been investigated.³³

The process dynamics and control of biodiesel production have also been addressed in the literature. Kariwala and Rangaiah (2012)³ developed a plantwide control (PWC) concept for a biodiesel production plant using control heuristics assisted with simulation. Shen et al. (2011)³⁴ studied the design and control of a biodiesel production process with phase separation and recycle. da Silva et al. (2021)³⁵ proposed key performance indicators for the evaluation of different plantwide control structures for a biodiesel production process. The process control of biodiesel production by reactive absorption has been also studied.^{33,36,37} Mjalli and Hussain (2009)³⁸ addressed the dynamics and control of a continuous reactor unit for biodiesel production. Brasio et al. (2016)³⁹ applied nonlinear model predictive control (NMPC) for the reaction section of a continuous biodiesel plant. They determined optimal profiles of the process variables using a nonlinear mechanistic model of the whole transesterification section. Benavides and Diwekar (2012)⁴⁰ developed an optimal control problem for biodiesel production in a batch reactor to maximize the final concentration of FAME by determining the optimal temperature profile. They extended their work and studied the effect of uncertainty in the reactor feed,⁴¹ and developed a two-layer optimization strategy to minimize operation time and maximize conversion in the reactor.⁴²

The aforementioned studies rely on commercial process simulators, mainly Aspen Plus⁴³ and Aspen HYSYS, ⁴⁴ and thus the model equations cannot be accessed. This is discussed in the comprehensive review by Chang and Liu (2010). ⁴⁵ Besides, Martín and Grossmann (2012)⁸ used a surface response methodology to model reactors and shortcut methods for distillation columns modeling in biodiesel production processes. Brasio et al. (2013)⁴⁶ developed first principle models for the reaction section and a simple decanter model based

on fixed split ratios. Others developed mechanistic models for the reaction section of oil transesterification processes only. 40,47–49 Farobie et al. (2015)⁵⁰ created an artificial neural network model by using experimental data, in order to predict biodiesel yield of a supercritical noncatalytic production reactor. However, we are unaware of any study in the literature that developed a detailed first-principle dynamic model of a complete biodiesel production plant with accessible and editable model equations that can be used as a digital twin and for model-based control applications like NMPC. Such a digital twin may be used to support the scaleup of biodiesel production processes and could improve cost-effectiveness in design and operation. Moreover, compared to models from commercial software, such modular models are needed for benchmark purposes and have a generic value for optimization and control applications, as they share features with many processes.

We present a rigorous mechanistic dynamic model of biodiesel production via homogeneous alkali-catalyzed transesterification of vegetable oils and provide the corresponding implementation open-source. We decouple unit operations and thermodynamic models. We model the reactors using material and energy balances and apply second-order elementary rate laws for kinetic modeling. We use the Material balance, phase Equilibrium, Summation, and Heat balance (MESH) equations for the separation units. Thermodynamic nonidealities are calculated based on the non-random two-liquid (NRTL) model⁵¹ and the Design Institute for Physical Properties (DIPPR) relations.⁵² We build the model framework in Modelica⁵³ as an open and powerful equation-based modeling language, which leads to modular and hierarchical building blocks that can be used for other chemical processes and fluids. Furthermore, we implement the same process in Aspen Plus v11⁴³ in order to compare the steady-state results of both models.

Moreover, in order to investigate the dynamic behavior of the plant, assess its controllability and provide a basic control level for future investigations, we design two plantwide decentralized control structures. Plantwide considerations are necessary due to the interconnected unit operations and recycle streams. For one PWC structure, we assume the availability of information-rich measurement configurations, including species concentration measurements, e.g., through process analytical technologies such as in-sito infrared or Raman spectroscopic technologies. ^{54,55} For the other PWC structure, we consider a structure that uses only conventional configuration with measurements for process quantities such as temperature, pressure, or flow rate, and thus matches current industrial practice. The design of the PWC structures and the tuning of their control loops must be based on the overall plant objectives. ^{35,56} Only few PWC methodologies are available, e.g., Luyben's heuristic-based methodology, ⁵⁷ self-optimizing control, ^{3,58-60} and the integrated framework of simulation and heuristics (IFSH). ^{3,61} We choose the IFSH methodology because it employs process simulation for assistance in using the heuristic PWC design steps. In addition, Konda et al. (2005) ⁶¹ and Kariwala and Rangaiah (2012) ³ provide detailed applications of the IFSH methodology.

Our work primarily addresses the lack of open-source and rigorous dynamic models of chemical processes for model-based applications. Specifically, the model is versatile, making it suitable for optimization and control applications, and also significant on its own due to its application potential. It encompasses the reaction, separation, and recycle aspects of a chemical plant, making it relevant to a wide range of processes. Furthermore, by applying the two PWC structures, assuming different measurement availability, we aim to demonstrate the importance of having dynamic models developed for model-based control and estimation as well as the application potential of advanced process analytics for process control purposes. Overall, the novelty of the work lies in providing an open-source dynamic model that can serve as a benchmark for the application of model-based techniques in chemical processes.

The remainder of the article is structured as follows. We first introduce the considered biodiesel production process and discuss the operating conditions. Then, we explain the considered assumptions behind the mathematical process model. Afterward, we discuss the developed PWC structures following the steps of the IFSH methodology. Before discussing the results of the plant dynamic simulation and control, we show how we simulate the plant under several scenarios to assess the performance of the PWC structures in terms of setpoint tracking and disturbance rejection. Finally, we draw conclusions about our contribution. We provide the full mathematical model in the supplementary material and the Modelica model including the PWC structures at permalink.avt.rwth-aachen.de/?id=135903.

2. Process description and operating conditions

We consider the homogeneous transesterification process of vegetable oil utilizing an alkali catalyst to produce biodiesel. This process is widely used in industrial production and is preferred over the acid-catalyzed and supercritical methods due to its faster reaction rate and lower methanol to oil ratios required under mild operating conditions.^{3,12} However, the alkali-catalyzed process is sensitive to the presence of water and free

fatty acids (FFA) in the feed. The presence of water may cause ester saponification under alkaline conditions, while FFA can react with the alkali catalyst to produce soaps and water.^{3,10} Saponification consumes the alkali catalyst and may cause the formation of emulsions, which can complicate the downstream recovery and purification of biodiesel. Hence, if the feed contains water and FFA levels beyond the maximum tolerance level, a pretreatment step is necessary to eliminate them. For our study, we assume the use of pretreated and refined vegetable oil.

Rapeseed oil, palm oil, and soybean oil are typical oil feedstocks. 6,7 The main constituents of these oils are the glycerides of the fatty acids. The glycerides of oleic fatty acid, mainly triglycerides, have been considered to represent the vegetable oil in many case studies of biodiesel production in literature because it is the main constituent of rapeseed oil and soybean oil as well as the second main constituent in palm oil after the glycerides of palmitic acid. $^{3,10,24,62-65}$ Chang and Liu $(2010)^{45}$ summarized the vegetable oil constituents used in several reported simulation models for biodiesel production plants. Triolein, the triglyceride of oleic acid, was mainly used to represent the oil feed in those models. Therefore, we use the glycerides of oleic acid to represent the vegetable oil. Based on Zhang et al. (2003), 10 Mint and El-Halwagi (2009), 24 and the summarized vegetable oil constituents in Chang and Liu (2010), 45 we use 95 wt% triolein and 5 wt% diolein as the nominal fed oil composition because it is a typical composition of oleic acid glycerides of vegetable oils. We use methanol for the transesterification of oil and sodium hydroxide solution (NaOH·H₂O) as the alkali catalyst, 3,10 due to their low prices and availability.

A process flowsheet of the considered biodiesel and glycerol production plant is depicted in Figure 1. The design of all process units and operating conditions are based on Zhang et al. (2003).¹⁰ Methanol and NaOH·H₂O are mixed before they are fed into the transesterifier, i.e., a continuous stirred tank reactor (CSTR). We feed the oil feed as well as the mixture of methanol and NaOH·H₂O into the CSTR without preheating. The outlets of the reactor are the biodiesel product, i.e., FAME, glycerol as a byproduct, the remaining reactants, and the catalyst solution. The products are then separated and purified in the separation section of the plant, and the reactants are recycled to the reactor. There are several configurations reported in the literature for the process separation section.^{3,10,24} We apply the design of Zhang et al. (2003)¹⁰ for the homogeneous alkali-catalyzed transesterification process. The main advantage of this design is that we can separate the unreacted oil from the biodiesel in a separate column, because methanol is separated in the methanol column before the decantation or water washing steps.

The optimal operating temperature of the CSTR for such a process is within the range of [55-75] °C.^{10,13,38} Following Zhang et al. (2003),¹⁰ we choose a nominal operating temperature of 60 °C. The homogeneous transesterification reaction could operate at atmospheric pressure. However, we operate the CSTR at 1.5 bar absolute pressure, by supplying nitrogen gas, to guarantee that methanol remains in the liquid phase at the nominal operating temperature as the bubble point of methanol at 1 bar is 65 °C.⁶⁶ We adopt the operating conditions that are optimal according to Zhang et al. (2003)¹⁰ and Abbaszaadeh et al. (2012)¹³ to achieve maximum conversion. We thus operate the CSTR at the optimal residence time of the reactor content of 1 h. The amount of the total methanol fed into the reactor is determined such that an optimal 6:1 methanol-to-oil mole ratio entering the reactor is achieved. The NaOH·H₂O is fed such that 2 wt% of NaOH in the mixture of methanol and NaOH·H₂O entering the reactor is preserved. We target 88% oil conversion with the 6:1 methanol-to-oil mole ratio and the preserved 2 wt% of NaOH ratio. We maintain the temperature of the reactor content by switching between hot and cold water as the input stream to the jacket of the CSTR.

The CSTR product stream is fed into the methanol column to recover methanol by a distillation process. The distillate, which has 99.5 wt% methanol as the nominal purity, is recycled to the transesterifier. The bottom product is cooled by a cooler that operates on water and fed to a wash column as the input raffinate. Water is fed as the input extract to the wash column to remove the polar species in the input raffinate. Glycerol, the dissolved NaOH, part of the methanol, and water are extracted from it to the fed water. The output raffinate is fed to the FAME column to separate the unreacted oil. The distillate is the biodiesel product which is mainly FAME and traces of water, monoglycerides, and methanol. The bottom product is recycled to the transesterifier after mixing it with the fresh-fed oil. The output extract of the wash column is sent to the glycerol purification section.

We follow the European specifications EN 14214⁶⁷ (cf. Table 1) to assess the quality of the produced biodiesel. The required low methanol concentration is achieved by adding the proper amount of water to the wash column. The oil glycerides concentration limits are guaranteed by achieving the required methanol-to-oil mole ratio entering the reactor.

We consider a biodiesel production rate of 17,120 kg/h corresponding to the average capacity of an industrial

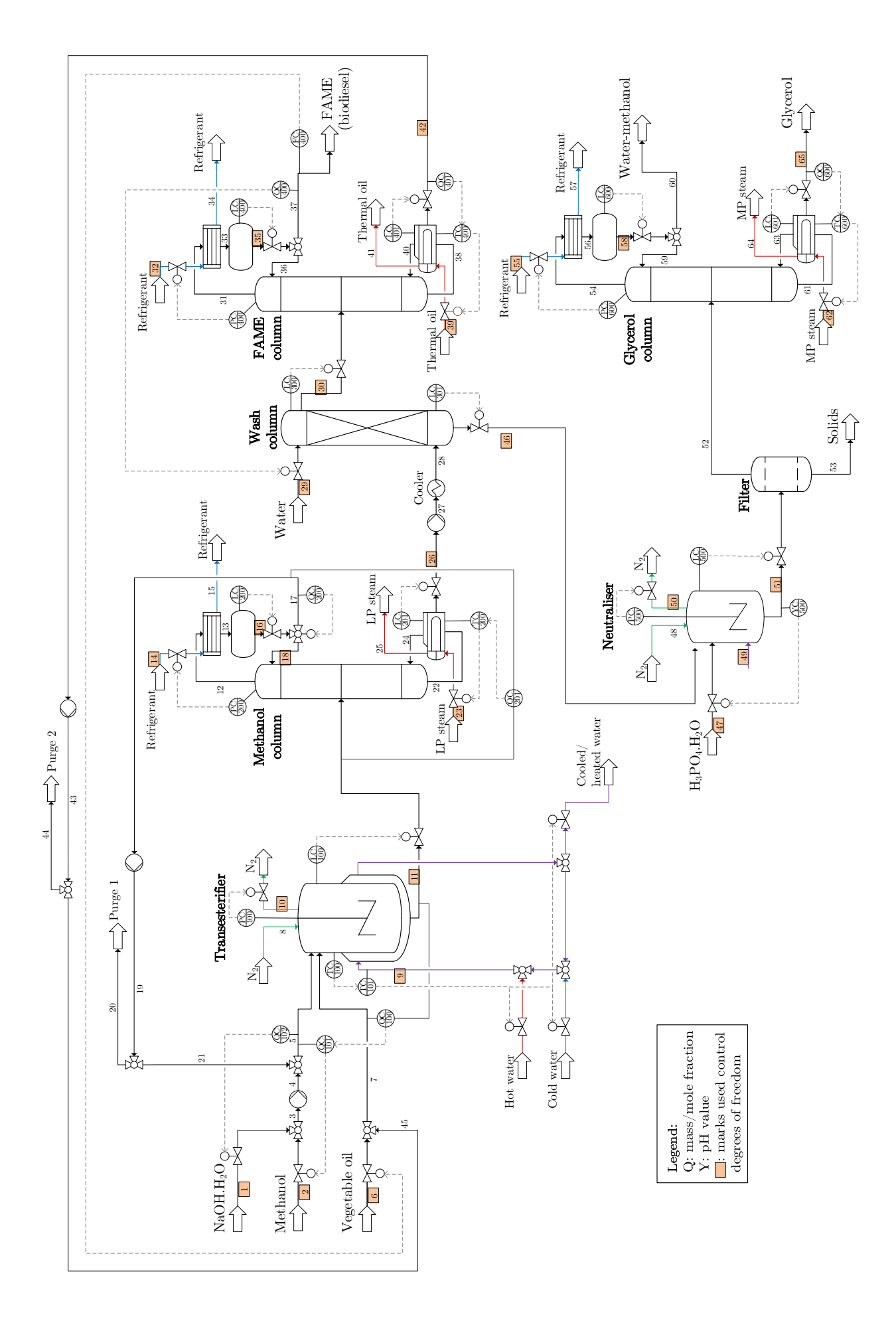


Figure 1: Process flowsheet with controllers of a biodiesel production plant by oil alkali-catalyzed transesterification. The shown control structure is for the PWC structure having information-rich measurement configurations available (PWC-A).

Table 1: Biodiesel specifications according to the European standard EN 14214.⁶⁷

| Ester content | $\geq 96.5 \text{ wt}\%$ |
|----------------|--------------------------|
| Triglycerides | $\leq 0.20 \text{ wt}\%$ |
| Diglycerides | $\leq 0.20 \text{ wt}\%$ |
| Monoglycerides | $\leq 0.80 \text{ wt}\%$ |
| Methanol | $\leq 0.20 \text{ wt}\%$ |
| Water | $\leq 0.05 \text{ wt}\%$ |
| Glycerol | $\leq 0.25 \text{ wt}\%$ |
| | |

biodiesel production plant in Germany (150,000 t/yr) according to the German Union for the Promotion of Oil and Protein Plants (UFOP).⁶⁸

The byproduct glycerol is also valuable, but needs to be neutralized and purified (cf. Figure 1). The output extract is fed to a neutralization reactor (neutralizer) to remove the dissolved NaOH species by the addition of phosphoric acid solution $(H_3PO_4 \cdot H_2O)$.²⁴ The resulting salt from the neutralization reaction is valuable too as it can be used as a fertilizer. We determine the amount of acid added such that the neutralized solution reaches a pH value of 2.5.⁶⁹ At this pH value, salt precipitation takes place and the formed solids can thus be filtered out in the filter unit. We assume that all of the dissolved NaOH is removed, and that the formed salt, which is monosodium phosphate (NaH₂PO₄), is completely precipitated. The liquid stream from the filter enters the glycerol column to purify glycerol from water and methanol. There are several grades of glycerol purity.⁷⁰ With the considered process design and operating conditions from Zhang et al. (2003),¹⁰ we target to have the pharmaceutical purity grade, which is 99 wt% glycerol,³ in the bottom stream of the glycerol column.

The methanol, FAME, glycerol, and wash columns have nine, five, five, and six separation stages, respectively. Low pressure (LP) steam, synthesized thermal oil, and medium pressure (MP) steam are used to heat the reboiler of the methanol, FAME, and glycerol columns, respectively. These utilities are suitable for the respective reboiler duties of each column. For the condensers of the three columns, refrigerants are the utility streams. The purge streams shown in the process flowsheet in Figure 1 are used to start up the plant. After starting the controller system (cf. Section 4), the plant is operated full automatically and the purge streams can thus be gradually decreased to zero.

3. Dynamic process model

We summarize in this section the chemical system involved in the process and the assumptions considered in the modeling. We provide the details in the supplementary material and the model implementation in Modelica at permalink.avt.rwth-aachen.de/?id=135903.

Ten species belong to the chemical system of the process model. Methanol, water, NaOH, triolein, diolein, and H₃PO₄ are the feeds. Monoolein is an intermediate educt and could be a constituent of the fed oil as well if the composition of the fed oil changes. The products are methyl oleate (FAME), glycerol, and NaH₂PO₄.

We model the transesterifier as an ideal (perfectly mixed) CSTR by energy and material balances. We assume for the alkali-catalyzed transesterification of oil with methanol, the well-studied and known reversible three-step reaction system in the literature. ^{12,28,62,71} We provide the reaction system and the rate law coefficients, and material and energy balances in the supplementary material. To account for the spatial distribution of the temperature of the reactor jacket, we model it as a series of equivalent CSTRs, by which the spatial dynamics of the jacket temperature are accurately determined. We assume a quasi-steady-state approximation for each jacket CSTR because their temperature dynamics are much faster than that of the reactor temperature. This can be validated by simulating and comparing the accumulation terms of the reactor and jacket temperatures. Moreover, such an assumption is often considered when modeling energy balances for jacketed CSTRs. ^{72,73}

For the distillation and wash columns, we use equilibrium models for each stage of the columns to determine species distributions among phases, flow rates, temperature profiles, etc. We consider the following assumptions when developing the equilibrium models: perfect mixing in vapor and liquid phases; the tray holdup is only due to the liquid phase (heavy liquid in the wash column) since the quantity of vapor (light liquid in the wash column) holdup is typically much smaller than the total holdup;⁷⁴ two-phase system in thermal and mechanical equilibrium; no heat of mixing; no heat losses to the surroundings; and the temperature dynamics of the column structure are neglected. The wash column is a liquid-liquid extraction process,

where the light phase is the raffinate stream. Since temperature dynamics on the column trays are faster than material dynamics, we adopt a quasi-steady-state approximation for their energy balances. This results in an index-1 differential-algebraic (DA) system as the outlet vapor (raffinate) flow from each tray can then be explicitly determined.⁷⁴

We model the heat exchangers by dividing them into segments. The thermal inertia from the metal wall between the two heat-exchanging streams is larger than that of the two streams. Therefore, we apply quasi-steady-state energy and steady-state material balances for the two heat-exchanging streams.⁷⁵ We neglect the axial heat of conductivity inside the metal wall.

We use the DIPPR temperature-dependent models for heat capacities to determine the molar heat capacities, enthalpies, entropies, and Gibbs free energies of the system's species in the solid, liquid, and vapor phases. Species' molar densities in the liquid and solid phases are also determined by the DIPPR correlations. All the coefficients of the DIPPR correlations are retrieved from DIPPR's Project 801 database. The values are unique for each species in each phase. The distillation columns operate at low pressure values. The transesterifier has the highest operating pressure value in the process, which is 1.5 bar. Therefore, we use the ideal gas equation of state to determine the molar densities in the vapor phase.

To account for the interactions among the polar species present in the system and describe the non-ideality in the liquid phase, we choose the NRTL⁵¹ as an activity coefficient model and the Racket equation⁷⁶ for determining the liquid mixture molar densities. To avoid minimizing the Gibbs free energy globally, we assume that the thermodynamics are such that the number of the existing phases is known. We thus use the isofugacity conditions for describing the liquid-liquid equilibrium (LLE), vapor-liquid equilibrium (VLE), and vapor-liquid-liquid equilibrium (VLLE). We use the extended Antoine correlation⁷⁷ to allow the description of the entire vapor pressure curves of the species when determining vapor pressures. Since the process operates at low pressures, the Poynting correction is neglected when computing equilibrium relations.

Albuquerque et al. (2020)⁶⁴ created databases of VLE, LLE and VLLE experimental data for the mixtures in the biodiesel production processes. They regressed the binary interaction parameters of the NRTL model for triolein, diolein, monoolein, methyl oleate, methanol, glycerol, and water. We use these values, which are provided in Table 6 and Table 7 in their publication.⁶⁴ We retrieve the parameter values of the remaining binary species from the database of Aspen Plus Physical Property.⁷⁸

4. Design of the PWC structures

To design the PWC structures, we apply the IFSH methodology, which decomposes the control system design process into several tasks at different levels in a vertical hierarchy of priorities. Table 2 summarizes the main steps involved in applying the IFSH methodology. Konda et al. $(2005)^{61}$ and Kariwala and Rangaiah $(2012)^3$ provided detailed applications of the methodology. We consider two structures that assume the availability of different measurement configurations. We first discuss the PWC structure that is based on information-rich measurement configurations, where inline product quality measurements such as species concentrations are available. This structure is motivated by the recent advances in process analytical technology, e.g., Infrared or Raman spectroscopy, for real-time process control applications. In the following, we refer to this PWC structure as PWC-A. We also provide a second PWC structure that is based on a more practical measurement configuration, in the sense of current industrial practice. Therein, only conventional measurements are available, i.e., real-time measurements for temperatures, pressures, flow rates, and pH (for the neutralizer output). We refer to this PWC structure as PWC-B. We illustrate the main steps of the conducted IFSH methodology for PWC-A, point out the differences for PWC-B, and summarize the two structures in Table 4. We tuned all control loops heuristically.

4.1. IFSH methodology for PWC-A

Step 1: Definition of PWC objectives

The PWC overall objectives of the plant include achieving the required production rate while preserving product quality specifications, stable operation of the plant, process and equipment constraints, safety concerns, and environmental regulations. We target to achieve a production rate of 17,120 kg/h of biodiesel while preserving its quality according to the standard EN 14214⁶⁷ as well as the pharmaceutical purity grade of the by-product glycerol, and operating below their thermal decomposition temperatures. The thermal decomposition temperature of glycerol is in the range of [150-180] °C.^{3,79-81} Therefore, we constrain the maximum allowable temperature in the reboiler of the glycerol column to 150 °C. The thermal decomposition temperature of FAME depends on the considered fatty acids in the oil. It is reported in the literature to be within a wide range of [250-350] °C.^{3,82,83} For the FAME of oleic fatty acid, methyl oleate, the range

starts from 325 °C.⁸² We consider a maximum allowable temperature in the reboiler of the FAME column to be 300 °C since we represent the fed oil as the glycerides of oleic acid.

To achieve the required recovery in the distillation columns as well as product purities, while constraining the reboiler temperatures to the thermal decomposition limits, the FAME and the glycerol columns operate at low pressures. The absolute pressure values at the top of the FAME and glycerol columns are designed to be 3 kPa and 2 kPa, respectively. We also target to attain the required oil conversion in the transesterifier, which is 88 %. In addition, we target to have 94 wt% of methanol recovery in the methanol column and 2 wt% of FAME loss in the bottom product of the FAME column. We thus design the PWC structure and its tuning based on those overall objectives.

Table 2: Main steps involved in the application of IFSH methodology, adapted from Konda et al. (2005)⁶¹ and Kariwala and Rangaiah (2012).³

| Step | Commonly conducted tasks |
|------|--|
| 1 | Definition of control objectives Achieve the required throughput and product quality Preserve stable operation and process constraints Involve safety and environmental constraints |
| 2 | Analyze the control degrees of freedom Identify the potential manipulated variables Involve material and energy streams Look-up tables exit for assistance in identification |
| 3 | Identification of throughput manipulator Identify the primary process path Selection of the throughput manipulator |
| 4 | Definition of quality controllers Identify primary quality manipulators Selection of the corresponding control loops |
| 5 | Controlling the more severe controlled variables Identify the manipulators of the more severe controlled variables Controlled variables involved in process, safety and environmental constraints |
| 6 | Controlling the less severe controlled variables Controlled variables involved in material inventory Levels for liquids and pressures for gases |
| 7 | Checking the material balances and remaining control degrees of freedom Material balance checks for the whole process as well as for its units Check if the control system performance can still be further enhanced |

Step 2: Control degrees of freedom analysis

We analyze the plant's control degrees of freedom (CDOF) to know what potential process streams we can manipulate to achieve the control objectives defined in Step 1. By following the flowsheet-oriented method of Konda et al. (2006),^{3,84} CDOF is defined as:

$$\label{eq:cdof} \text{CDOF} = N_{\text{streams}} - N_{\text{restraining}} - N_{\text{redundant}} \,.$$

The total number of streams (including material and energy streams) $N_{\rm streams}$ is 65 (cf. numbered streams in Figure 1). The number of process streams that cannot be manipulated due to their dependency on other streams $N_{\rm restraining}$ is 25. The total number of process streams that need not be manipulated $N_{\rm redundant}$ is nine because each distillation column has three redundant streams. 3,84 Table 3 provides the restraining and redundant number of streams of each process unit. It is easy to compute $N_{\rm streams}$, given a process flowsheet. However, $N_{\rm restraining}$ and $N_{\rm redundant}$ depend on the nature of the unit and its operation. Consequently, they are determined based on the theoretical and operational knowledge of any given unit or combination of units (such as a distillation column with a condenser, reflux drum, and reboiler) in a process. 3,84 Both terms are thus characteristic of a given unit and remain the same irrespective of whether the unit is a standalone or an integral part of a process. Therefore, once determined, they need not be recomputed and can be accessed from

look-up tables such as the tables in Konda et al. $(2006)^{84}$ and Kariwala and Rangaiah $(2012)^{.3}$ Nevertheless, it should be noted that the value of $N_{\text{restraining}}$ is contingent on the number of streams considered around a unit operation and whether holdups are modeled or not. For instance, if all streams are considered around a unit operation without modeling material holdup, then $N_{\text{restraining}}$ would be one. Consequently, it may differ from the values listed in the aforementioned look-up tables, depending on whether all material and energy streams are taken into account or not. As a result, we obtain 31 CDOF as a maximum limit for the manipulated variables that we could consider to control the plant.

Table 3: Restraining and redundant number of streams of process units according to Konda et al. (2006)⁸⁴ and Kariwala and Rangaiah (2012).³

| Unit operation | Number of units | $N_{\text{restraining}}$ per unit | $N_{ m redundant}$ per unit |
|----------------------------------|-----------------|-----------------------------------|-----------------------------|
| CSTR | 2 | 1 | 0 |
| Distillation column [†] | 3 | 0 | 3 |
| Wash column | 1 | 0 | 0 |
| Condenser | 3 | 2 | 0 |
| Reboiler | 3 | 1 | 0 |
| Distillate drum | 3 | 0 | 0 |
| Cooler | 1 | 1 | 0 |
| Filter | 1 | 1 | 0 |
| Pump | 4 | 1 | 0 |
| Mixer | 3 | 1 | 0 |
| Splitter | 5 | 1 | 0 |
| Total | | 25 | 9 |

[†] Excluding condensers, reboilers, distillate drums, and splitters for reflux.

Step 3: Identification of throughput manipulator

We identify the throughput manipulator (TPM) of the plant, by determining the primary process path from the main raw material to the main product. For our process, it is the fed oil to biodiesel product path. Therefore, we control the desired production rate of biodiesel by setting the flow controller FC|400, where the manipulated variable (MV) is the fed-oil flow rate, as shown in Figure 1.

Step 4: Definition of quality controllers

In this step, we define the quality controllers for the FAME and glycerol products. By introducing fresh water into the wash column, glycerol, NaOH, and methanol are extracted from the raffinate, which is the feed of the biodiesel purification unit (FAME column). We thus control the concentration of methanol in the biodiesel product by manipulating the input water to the wash column. Therefore, we set the quality controller QC|400, where we assume the mass fraction of methanol in the biodiesel product is measured and use it as its controlled variable (CV). The flow rate of the input water to the wash column is its MV.

Higher reaction conversions in the transesterifier mean lower unreacted oil entering the FAME column. We thus control the oil glycerides limits in the biodiesel product by achieving the required oil conversion in the transesterifier. High oil conversions are achieved by feeding enough excess methanol to the transesterifier. Thus, we set a cascade controller, where the CV of its primary loop (QC|100) is the oil conversion, and the CV of its secondary loop (QC|101) is the methanol-to-oil mole ratio of the streams entering the transesterifier. The MV of the controller is the flow rate of the input methanol to the plant. This cascade control loop is shown in Figure 1.

Achieving the required grade of glycerol product is a single-end composition control case for the glycerol column. Hence, we control glycerol purity by implementing a cascade controller, with purity as the primary CV in QC|600 and the reboiler temperature of the glycerol column as the secondary CV in TC|600. The controller TC denotes temperature controller. Its MV is the flow rate of the input MP steam into the reboiler. We set the maximum reboiler temperature of the controller to the thermal decomposition temperature of glycerol.

Step 5: Controlling the more severe controlled variables

In the IFSH methodology, the more severe CVs are the variables associated with process constraints, e.g., operating and equipment constraints, safety concerns, and environmental regulations.

To minimize losing FAME in the recycled bottom product of the FAME column, we control its recovery by inputting adequate reboiler duty. We thus set a cascade controller, where the CVs of its primary (QC|401) and secondary (TC|400) control loops are the FAME mass fraction in the bottom product and the reboiler temperature, respectively. Its MV is the flow rate of the input thermal oil into the reboiler. We set the maximum limit of the reboiler temperature in the controller to the considered thermal decomposition temperature of methyl oleate.

We achieve the nominal purity of the recycled methanol from the methanol column to the transesterifier by manipulating the flow rate of the column reflux by QC|200. In addition, similar to the FAME column recovery, we target to recycle most of the methanol in the methanol column. Therefore, we control its recovery by also implementing a cascade controller. The CVs of its primary (QC|201) and secondary (TC|200) control loops are the column recovery and the reboiler temperature, respectively. Its MV is the flow rate of the input LP steam into the reboiler.

The nominal temperature of the transesterifier content is maintained by exchanging heat with the flowing medium in the reactor jacket. The jacket medium flows through an external loop in which cold water, hot water, and purge valves open or close according to the required heating or cooling duties of the jacket/reactor system. We model this external loop by considering a temperature change ΔT_{Jacket} of the jacket medium after passing through a pseudo heat exchanger. This way, we control the heating or cooling modes of the reactor by one control loop with one MV. After the jacket medium exits the jacket, it changes its temperature by ΔT_{Jacket} value after passing through the external heat exchanger, to enter again the jacket. We thus control the reactor temperature by a cascade controller, where the CVs of its primary (TC|100) and secondary (TC|101) control loops are the temperatures of the reactor content and the water medium entering the jacket, respectively. Its MV is ΔT_{Jacket} with extreme values of ± 10 °C.

Finally, we set QC|102 to control the mass fraction of NaOH in the mixture of methanol and NaOH \cdot H₂O entering the transesterifier by manipulating the NaOH \cdot H₂O feed flow rate.

Step 6: Controlling the less severe controlled variables

Less severe CVs are the variables associated with the material inventory. These CVs are the pressures at the top of the three distillation columns and in the reactors, and the liquid levels in process units. We set pressure controllers (PC) to control column pressures (PC|200, PC|400, and PC|600) by manipulating the refrigerant flow rates entering the condensers, and reactor pressures (PC|100, and PC|500) by manipulating the N₂ gas flow rate leaving the reactors. The level controllers (LC) control liquid levels in the transesterifier (LC|100), neutralizer (LC|500), reflux drums (LC|200, LC|400, and LC|600), reboilers (LC|201, LC|401, and LC|601), and the bottom and top sections of the wash column (LC|300, and LC|301), by manipulating the flow rates of their respective output streams. We implement variable level control for the transesterifier to avoid snowball effects in the recycle loops. Recycle systems tend to exhibit large variations in the magnitude of their recycle flows in the presence of small disturbances. This high sensitivity of the recycle flow rates is known as the snowball effect. Hence, according to Luyben et al. (1999), so we implement the variable level control as a cascade controller where the outer loop controls the desired residence time of the reactor content to 1 h and sends level setpoints to the LC in the inner loop. In addition, we add a pH controller (YC|500) for the outlet stream of the neutralizer, where its MV is the flow rate of the H₃PO₄ · H₂O feed stream.

Step 7: Checking the material balances and remaining CDOFs

In the final steps of the IFSH framework, we check the material balances in the plant as well as in its single units by simulating the process. We also check if we can use the remaining CDOFs, which are five (we used 26, cf. stream numbers marked in orange rectangles in Figure 1), to enhance the performance of the control system. Based on the defined PWC objectives and structure, no additional control loops are needed.

4.2. IFSH methodology for PWC-B

To design the PWC-B structure, we perform the same steps of the IFSH methodology as for the case of the PWC-A, except for the quality controls. Since quality measurements for product and educt streams are not available, we replace the quality controllers with flow rate ratio controllers (RC). We use the steady-state values from PWC-A for determining and setting the ratio values in these controllers.

For the transesterifier, we replace QC|100 and QC|101 with RC|100, where the methanol feed flow rate is manipulated to maintain a fixed ratio between the flow rates of the total methanol and NaOH· H_2O mixture, and the oil entering the transesterifier. Likewise, we manipulate the NaOH· H_2O feed flow rate through RC|101 instead of QC|102 by maintaining a fixed ratio between the flow rates of the NaOH· H_2O

feed, and the methanol and $NaOH \cdot H_2O$ mixture entering the transesterifier.

For the methanol column, we remove QC|200 and fix the design setpoint for the reflux ratio, and replace QC|201 with RC|200. Similar to PWC-A, the MV of RC|200 is the setpoint of TC|200. RC|200 changes its MV to preserve a fixed ratio between the flow rates of the output bottom and the input feed of the methanol column.

We replace QC|400 in the FAME column with RC|300 to determine the water feed flow rate into the wash column. RC|300 maintains a fixed ratio between the flow rates of water feed and input raffinate into the wash column. RC|400 manipulates the setpoint of TC|400 to maintain a fixed ratio between the flow rates of the output distillate and the input feed of the FAME column.

Similar to the methanol column, RC|600 preserves a fixed ratio between the flow rates of the output bottom and the input feed of the glycerol column by manipulating the setpoint of TC|600.

We provide the process flowsheet for PWC-B in the supplementary material. The used CDOF for this case is 25 because we remove QC|200 and fix the reflux ratio in the methanol column.

PWC-B can be configured in other ways. A common configuration is to use internal temperature controllers for the distillation columns instead of the cascade ratio controllers. However, with the plant disturbances we introduce (cf. Section 5), we expect difficulties to track the product purity setpoints (particularly methanol impurity and glycerol purity) for either configuration.

We summarize the two PWC structures in Table 4.

Table 4: Comparison of PWC-A and PWC-B structures.

| | PWC-A | PWC-B |
|--------------------------------------|--|---|
| Available measurements | Temperature, pressure, flow rate, pH, and concentration | Temperature, pressure, flow rate, and pH |
| Used CDOF | 26 | 25 (QC 200 is removed) |
| Material inventory control | Pressure and level controllers for all unit operations | Same as PWC-A |
| Production rate control | By oil feed flow rate (TMP) | Same as PWC-A |
| Methanol feed flow rate manipulation | Determined by cascade control of the reaction conversion in the transesterifier | Determined by a ratio controller with the flow rate of the feed oil |
| Catalyst feed flow rate manipulation | Determined by controlling the NaOH concentration in the methanol-catalyst mixture entering the transesterifier | Determined by a ratio controller with the flow rate of the methanol-catalyst mixture entering the transesterifier |
| Water feed flow rate manipulation | Determined by controlling methanol impurity in the biodiesel product | Determined by a ratio controller with the flow rate of the raffinate entering the wash column |
| Acid feed flow rate manipulation | For pH control in the neutralizer | Same as PWC-A |
| Reboiler duties manipulation | For controlling products purities and column recoveries | Determined by ratio controllers of the column distillate/bottom with feed flow rates |

5. Simulation scenarios for assessment of process dynamics and PWC performance

We first let the plant reach a steady state, after initializing its dynamic model and applying the developed PWC structures while gradually decreasing the purge streams to null. To study its dynamic behavior as well as the performance of the applied PWC structures, we introduce several process disturbances and setpoint tracking scenarios that are commonly found in literature and practice. We perform simulations under the

following seven scenarios (one at a time), corresponding to one production rate setpoint change (ST) and six alternative disturbances (SD):

- ST1: setpoint change of biodiesel production rate. The red-dashed line in Figure 5f shows the setpoint of the biodiesel production rate over time. The setpoint changes at 1 h over 4 h while being ramped by $\pm 10\%$ from its nominal value until it returns to it at 5 h. Such setpoint changes could be required when the targeted plant capacity changes in accordance with product amount demand. Plant capacity flexibilization for optimizing production costs is also a potential reason for such changes.
- SD1: decrease in the rate coefficients of the transesterifier forward reactions by 20% at time 8 h (t_k). This scenario could occur when the quality or type of the fed oil changes. Also, fouling in the reactor is a potential reason for such a disturbance.
- SD2: 30% drop in the overall heat transfer coefficient in the transesterifier reactor/jacket system at time 13 h ($t_{\rm U}$). This could occur when fouling in the reactor/jacket system is present.
- SD3: trays fouling and wear in the methanol column. As a result, their separation efficiency decreases. We model this disturbance by eliminating two trays of the column at time 15 h (t_{tray}). Trays fouling and wear are common and occur in practice.
- \bullet SD4: column flooding in the FAME column. We model this disturbance by omitting two trays at time 21 h over 0.5 h.
- SD5: foaming in the glycerol column. We model this disturbance by omitting two trays at 25 h over 0.5 h.
- SD6: change in the composition of the fed oil from [0.95 wt% triolein, 0.05 wt% diolein, 0 wt% monoolein] to [0.8 wt% triolein, 0.1 wt% diolein, 0.1 wt% monoolein]. We introduce this disturbance at 27 h (t_{feed}) before the plant reaches a new steady state at 35 h. This disturbance occurs when the fed oil type or quality changes.

The scenarios are introduced at the times depicted in Figure 2. The time points are selected to ensure that new steady states are reached in between scenarios. However, it is worth noting that some of the introduced events, such as fouling in the reactor/jacket system of the transesterifier or tray fouling in the methanol column, may require significantly longer durations to manifest in practical situations. Nevertheless, for the purpose of studying the dynamic behavior of the process units under such circumstances, we intentionally introduce these disturbances at the specified time points.

6. Simulation results for validation of the dynamic model and assessment of the PWC structures

We implement the process model with the developed PWC structures using the object-oriented modeling language Modelica.⁵³ The model components can be used with different fluids because we decouple the component equations (e.g., mass and energy balance equations) from thermodynamic property equations (e.g., calculation of specific enthalpy or activity coefficient). The PID controller equations of the PWC structures are part of the differential-algebraic system of equations within the model. We simulate the process in Dymola 2020⁸⁶ and use the implicit, multi-step Differential Algebraic System Solver (DASSL).⁸⁷

Due to the large number of process variables and control loops present, it is impractical to show the profiles of each process variable and every control loop. Hence, we analyze the dynamic behavior of the plant and the performance of control structures in a plantwide context. We first provide profiles for some process variables of the three main types of unit operations involved in the process, simulated for the case of applying PWC-A. These units are the CSTRs, distillation columns, and a wash column.

We then study the performance of the two developed PWC structures and compare them by providing and discussing the profile of the process feed and product flow rates, the reboiler duties, as well as some of the more severe and product quality CVs in the plant. We provide the dynamic profiles of the remaining variables and control loops in the supplementary material. In addition, based on Vasudevan and Rangaiah (2010)⁸⁸ and Kariwala and Rangaiah (2012),³ we provide three measures to quantitatively compare the dynamic performance of the two PWC structures. The performance measures correspond to the overall settling time, the total plant accumulation, and the total deviation from the production target.

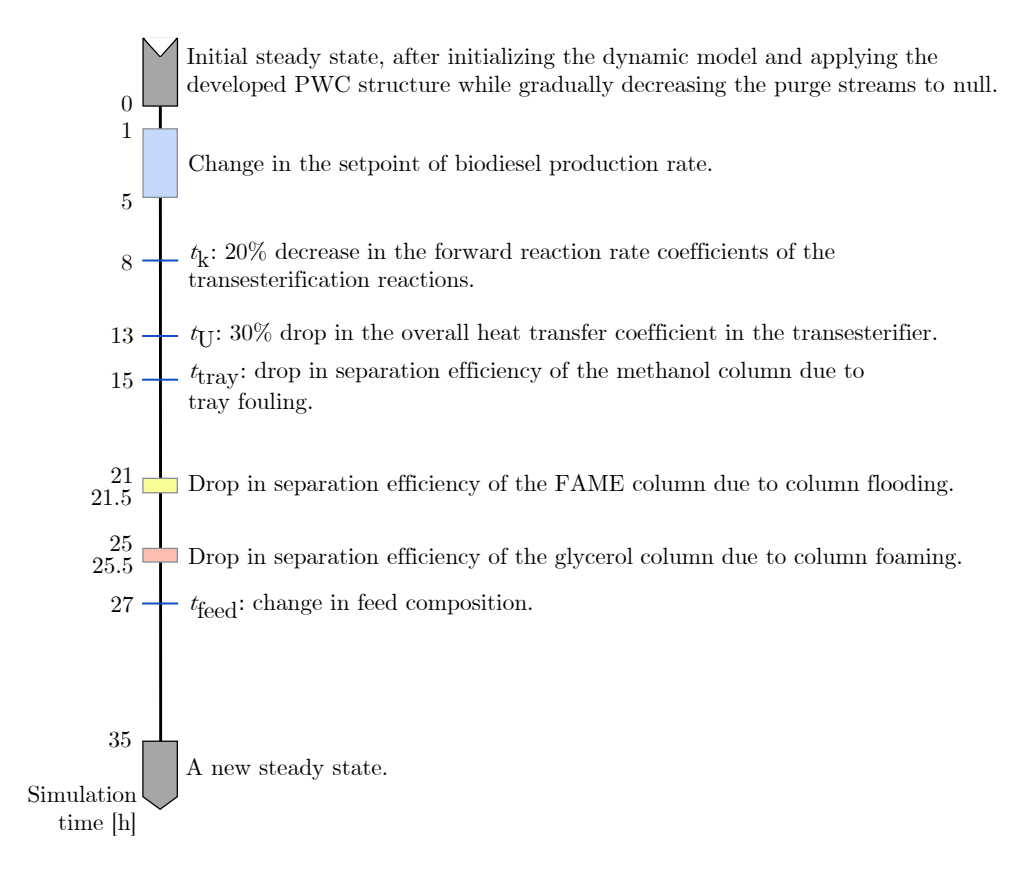


Figure 2: Changes in the setpoint of biodiesel production rate and plantwide disturbances over the simulation time of the plant.

We also compare the steady-state simulation results of the model with that of Aspen Plus. We implemented a similar process with the same inputs and operating conditions in Aspen Plus v11,⁴³ which we also provide at permalink.avt.rwth-aachen.de/?id=135903. The main models used in the Aspen Plus process are the RCSTR, RadFrac, and Extract for the transesterifier, the distillation columns, and the wash column, respectively. We selected the NRTL model as the base method with the default Route ID for properties. We provide results for mole fraction, flow rate, and temperature profiles in tables in the supplementary material for each of the aforementioned three main unit operations comparing both models. The results are very close, demonstrating the validity of our model. Nonetheless, there are some differences in the results due to mainly the different used numerical integration schemes.

6.1. Dynamic behaviour of the main unit operations

Figure 3 shows the net reaction rate profiles of the considered three transesterification reactions in the transesterifier. In the blue-shaded region, we perform setpoint changes in the biodiesel production rate. In this region, the reaction rates follow the feed flow rate profiles, which are provided in Figures 5a–e. At t_k , a drop in the forward reaction rate coefficients results in a proportional drop in the reaction rates. The disturbance at t_U (drop in overall heat transfer coefficient in the transesterifier) does not affect the reaction rates. The disturbance in the light-brown region has also no effect because there are no recycle streams from the glycerol column to the transesterifier. In the last disturbance at t_{feed} , because the composition of the fed oil has more diolein and less triolein, the triolein transesterification (reaction (1)) shifts more toward the reverse reaction direction. Therefore, its net reaction rate decreases. For diolein transesterification (reaction (2)), although the fed oil has more diolein, the net reaction rate decreases because more monoolein is fed, which drives the reaction more into the backward direction. For the last reaction, since monoolein input increases, the reaction is shifted to the forward direction, and thus the net reaction rate increases as indicated in Figure 3 for reaction (3).

For the distillation columns, we provide the temperature profile of the methanol column in Figure 4a. The temperature values increase in the direction from stage one, the condenser, to stage eleven, the reboiler. At t_k , due to the drop in the forward reaction rate coefficients, less methanol reacts in the transesterifier and thus more enters the column. Therefore, lower reboiler temperatures are needed to attain the required column recovery and methanol purity in the distillate stream. This explains the decrease in the temperature

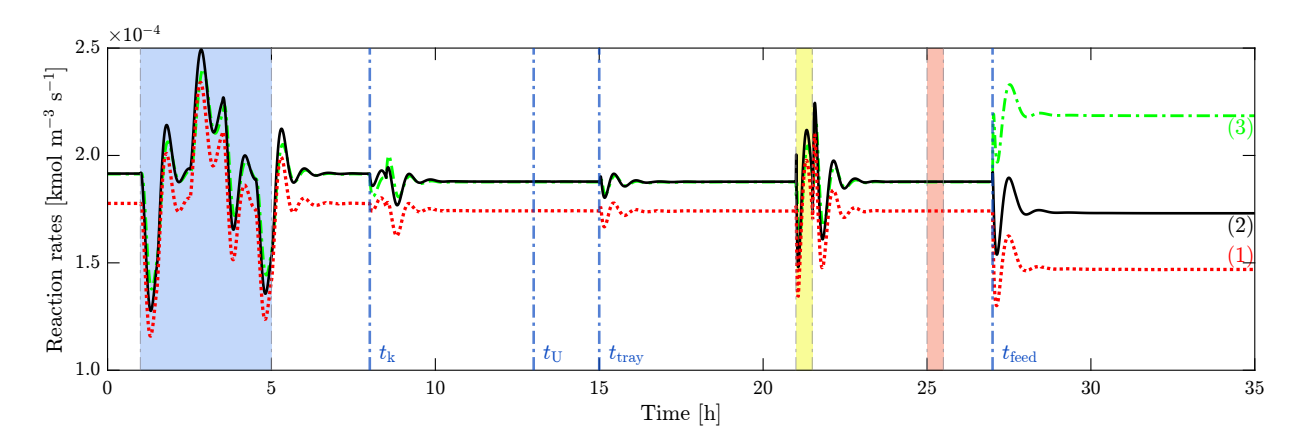
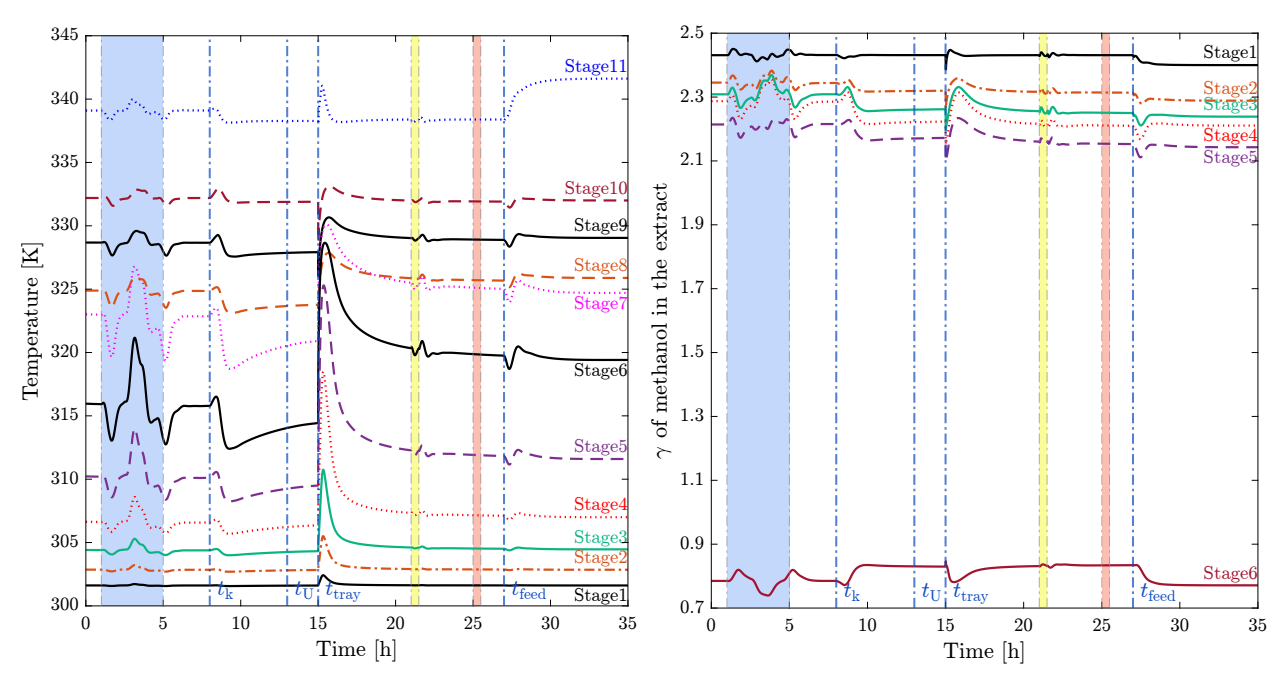


Figure 3: Net reaction rate profiles of the three alkali-catalyzed transesterification reactions in the transesterifier, simulated under the disturbances and setpoint changes provided in Figure 2. The reactions are indicated by the number of their respective rate coefficient subindex j in equations (S1a), (S1b), and (S1c) in the supplementary material. The dotted-red, solid-black, and dashed-dotted-green lines correspond to reactions (1), (2), and (3), respectively.

values in the figure. At $t_{\rm tray}$, the number of trays in the column is decreased by two. Therefore, higher temperature values are needed to preserve the required purity and recovery. However, the purity controller increases the reflux rates and thus the temperature values decrease back to their previous steady-state values. In the last disturbance, due to the increase in the reaction rate of reaction (3), more methanol reacts in the transesterifier, thus, less fraction enters the column. Therefore, higher temperature values are needed to keep the desired recovery and purity. This can be seen in the figure at $t_{\rm feed}$, where the temperature values increase to reach a new steady state.



(a) Temperature profile in the methanol column. Stage 11 (b) Methanol activity coefficient (γ) profile in the extract is the reboiler. phase of the wash column. The raffinate enters at stage 6.

Figure 4: Process variable profiles in two main unit operations of the process, simulated under the disturbances and setpoint changes provided in Figure 2.

In Figure 4b, we show the activity coefficient profile of methanol in the extract phase in the wash column. The values of the activity coefficient decrease by going from stage one to stage six. The raffinate enters the column at the sixth stage. In the final disturbance at $t_{\rm feed}$, more glycerol is being produced in the transesterifier, since monoolein mass fraction in the fed oil increases. Therefore, a higher amount of glycerol enters the wash column and is extracted to the extract phase. Glycerol is a polar species and higher amounts

of it increase the attractive forces among the polar species in the mixture. Therefore, the activity coefficient values of the polar species decrease in the extract phase and so does that of methanol, as shown in the figure.

6.2. Performance of the PWC structures

We provide the results for all disturbances in the supplementary material. In this section, we provide the profiles only for scenarios ST1, SD1, and SD6. The disturbances of tray fouling in the methanol column SD3 and flooding in the FAME column SD4 have less interpretable results. For SD3, higher reboiler duties in the methanol column are required to maintain the desired methanol recovery and purity in the column. For SD4, higher mass fraction of monoolein impurity is present in the biodiesel product. However, it stays significantly below its maximum limit. There are no effects on the process dynamics for the drop in the overall heat transfer coefficient scenario SD2. Also, since there are no recycles from the glycerol purification section, the disturbance of foaming in the glycerol column SD5 does not affect the plant.

6.2.1. Scenario ST1: Change in biodiesel production rate setpoint

Figure 5 provides the results for the scenario ST1 for both PWC structures, PWC-A (solid-black curves) and PWC-B (dashed-dotted-green curves). The biodiesel production rate is the plant throughput. Its setpoint is shown in the red-dashed line in Figure 5f. The flow rates of all feeds are MVs. The oil feed flow rate (Figure 5c) is the TPM and is manipulated based on the changes in the biodiesel production rate setpoint. For both PWC structures, its profiles look similar because they have the same FC|400. For PWC-A, the methanol (Figure 5a) and NaOH \cdot H₂O (Figure 5b) feed flow rates are manipulated according to the required oil conversion (88%) in the transesterifier and NaOH mass fraction in their fed mixture stream, respectively. For PWC-B, they are manipulated according to RC|100 and RC|101, respectively, and thus follow the oil feed flow rate. Therefore, for both PWC structures, the flow rates of the three transesterifier feeds are proportional to that of the biodiesel production rate.

Glycerol product flow rates (Figure 5g) are proportional to that of biodiesel because they are produced in the same reaction direction. Since the addition of acid is dependent on the fed $NaOH \cdot H_2O$, its and the formed solids flow rates (Figures 5e and 5i, respectively) are also proportional to that of biodiesel, for PWC-A and PWC-B. The profiles of water-methanol product (Figure 5h) follow the profiles of $NaOH \cdot H_2O$ and methanol feeds. Therefore, they are also proportional to the produced biodiesel profile.

For PWC-B, since the addition of water feed (Figure 5d) is controlled by RC|300, its flow rate profile is proportional to that of the fed raffinate into the wash column. Thus, it is proportional to the produced biodiesel flow rate. On contrary, for PWC-A, when low production rates are required, higher water flow rates are fed to the wash column and vice versa. Lower production rates of biodiesel result in lower formation rates of FAME in the transesterifier. Therefore, the outlet stream of the transesterifier will have higher fractions of methanol, since the consumption rate of methanol is proportional to the formation rate of FAME. As a result, for PWC-A, more water will be needed for methanol extraction in the wash column to achieve the required methanol concentration in the biodiesel product, which is controlled by QC|400.

In Figures 5j-l, the reboiler duties are proportional to the production rate of biodiesel, as the stream flow rates in the reboiler units are proportional to it.

For PWC-A, all quality controllers (Figures 5m–p) are able to return the corresponding CVs to their setpoints while achieving tight control for methanol recovery and glycerol purity. We set the setpoint for methanol mass fraction in the biodiesel product to 0.0013. While there is no direct quality control in PWC-B, the indirect control for the quality CVs by ratio controllers can return these CVs to their corresponding setpoints. Nevertheless, RC|600 is unable to preserve the required purity of the final product glycerol at all times, reflecting the effects of changes in production load.

6.2.2. Scenario SD1: 20% decrease in the forward reaction rate coefficients

Figure 6 provides the results for the scenario SD1 for both PWC structures. For PWC-A, more NaOH · $\rm H_2O$ (Figure 6b) starts to enter the plant to compensate for the drop in the reaction rate coefficients at t_k and preserve the required oil conversion in the reactor. Methanol feed flow rate (Figure 6a) increases then returns to its previous steady-state value, because its needed amount to achieve the required oil conversion is compensated by the increase in NaOH · $\rm H_2O$ while preserving the required methanol recovery and purity in the methanol column. For PWC-B, since the forward reaction rates decrease, less methanol reacts in the transesterifier and thus more enters the methanol column. With a fixed ratio in RC|200, the required methanol recovery cannot hence be achieved. This is shown by the drop in the dashed-green curve in Figure 6m. However, its purity increases (Figure 6n) because more methanol enters the column. Since less methanol

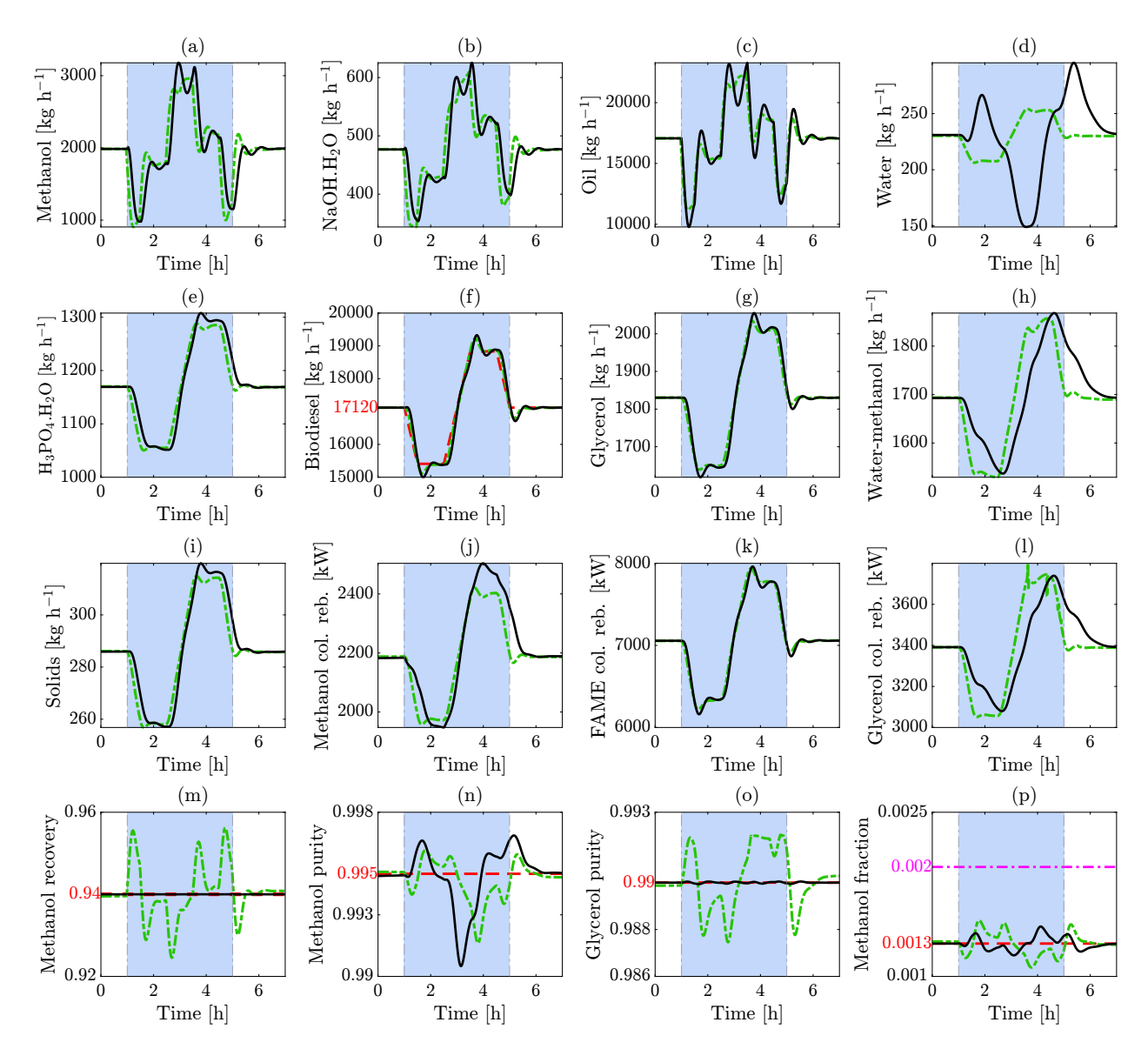


Figure 5: The profiles for the scenario ST1 of the change in biodiesel production rate setpoint as provided in Figure 2. The load changes take place in the blue-shaded region. (a)–(e): feed mass flow rates. (f)–(i): product mass flow rates. (j)–(l): reboiler duties. (m): methanol recovery in the methanol column. (n): methanol mass fraction in the methanol column distillate. (o): glycerol mass fraction in the glycerol column bottom. (p): methanol mass fraction in the biodiesel product. The solid-black and dashed-dotted-green curves are for the results of PWC-A and PWC-B, respectively. The dashed-red and dashed-dotted-magenta lines are the setpoints and bounds, respectively.

is recovered in the methanol column, more methanol feed is fed to preserve the ratio in RC|100 between the total oil, and methanol and $NaOH \cdot H_2O$ mixture entering the transesterifier. This also explains the increase in $NaOH \cdot H_2O$ feed flow rate, which is manipulated by RC|101 in the case of PWC-B. Since both PWC structures have the same FC|400, they have similar behavior in controlling the desired biodiesel production rate (Figure 6f), and thus in manipulating the fed oil flow rates (Figure 6c).

Since more methanol leaves the transesterifier due to the decrease in the forward reaction rates, more enters the wash column and thus appears in the distillate of the FAME column. To preserve the required methanol fraction in the biodiesel product, more water enters the wash column for the PWC-A, as can be seen in Figure 6d. However, the ratio controller RC|300 in PWC-B manipulates the fed water flow rate according to a preserved ratio with the fed raffinate and thus fails to feed a sufficient amount of water to preserve the required setpoint of methanol in the biodiesel product. This is shown in Figure 6p, where the dashed-green curve increases to approach the maximum allowed mass fraction of methanol.

For both PWC structures, the increase in NaOH \cdot H₂O flow rates leads to an increase in the needed amount of acid for neutralization. As a result, more water-methanol and solids products (Figures 6h and 6i, respectively) are produced. By preserving the required purity of the glycerol product (Figure 6o), its flow rate profile (Figure 6g) should follow the controlled biodiesel production rate because it is formed proportionally to FAME formation. This is the case for PWC-A. In contrast, for PWC-B, since more water is fed to the glycerol purification section, the RC|600 increases the produced glycerol product while decreasing its purity. Therefore, in this disturbance scenario, PWC-B fails to achieve the required glycerol product purity, track the setpoint of methanol mass fraction in the biodiesel product (rather shifts to its upper abound), and preserve the desired methanol recovery in the methanol column.

For both PWC structures, higher reboiler duties are needed in the methanol and glycerol columns (Figures 6j and 6l, respectively) because more water enters the columns, thus increasing the enthalpies of vaporization in the reboilers. Since for PWC-B, the required oil conversion is not achieved by the addition in the fed $NaOH \cdot H_2O$ as for PWC-A, more residual oil, especially triolein, leaves the transesterifier and ends in the reboiler of the FAME column. This increases the heat duty in the reboiler as shown in Figure 6k.

6.2.3. Scenario SD6: Change in the oil feed composition

Figure 7 provides the results for the scenarios SD6 for both PWC structures. In this last disturbance, we increase the diolein and monoolein mass fractions in the fed oil. Therefore, less methanol and NaOH \cdot H₂O fraction are needed to achieve the same oil conversion. In PWC-A, since the oil conversion is directly controlled by QC|100, the fed methanol and NaOH \cdot H₂O flow rates are adjusted accordingly and hence decreased. This also explains the drop in the fed acid flow rate (Figure 7e) and thus the formed solids (Figure 7i) for PWC-A. In contrast, in the case of PWC-B, since there is no direct control for the oil conversion in the transesterifier, more methanol is present in the reactor and thus fed into the methanol column. Therefore, the methanol recovery decreases, and its purity increases (Figures 7m and 7n, respectively). Hence, both methanol and NaOH \cdot H₂O feed flow rates increase as explained in the previous disturbance scenario for PWC-B.

Increasing the diolein and monoolein mass fractions in the fed oil results in an increase in glycerol formation in the transesterifier (see reaction rates in Figure 3). This explains the increase in glycerol product flow rates in Figure 7g for both PWC structures. As aforementioned, glycerol increases the polarity of the extract mixture in the wash column. Therefore, the activity coefficient value of methanol in the extract phase decreases (see Figure 4b). Thus, less water is needed for methanol extraction. This explains the decrease in the fed water flow rate for PWC-A in Figure 7d. On the other hand, since the fed water flow rate is manipulated by a fixed ratio in RC|300 for PWC-B, it increases with the increase of the input raffinate to the wash column. The input raffinate increases because more glycerol is being produced while having the same amount of the produced biodiesel.

The produced water-methanol follows the profiles of the fed water into the wash column, acid, and NaOH \cdot H₂O. For PWC-A, less water, acid, and NaOH \cdot H₂O are fed, which is the opposite for PWC-B. This explains the product flow rate profiles for both PWC structures in Figure 7h.

In the case of PWC-B, increasing the diolein and monoolein mass fractions in the fed oil, while also increasing the methanol and $NaOH \cdot H_2O$ feeds flow rates, results in an increase in the oil conversion. Therefore, less residual oil ends in the reboiler of the FAME column. This explains the decrease in the reboiler duty of the FAME column in Figure 7k for PWC-B. On contrary, it increases for PWC-A, because the overall amount of residual oil increases for the same desired oil conversion in the transesterifier. For both PWC structures, the reboiler duties of the methanol and glycerol columns (Figures 7j and 7l, respectively) follow the profiles

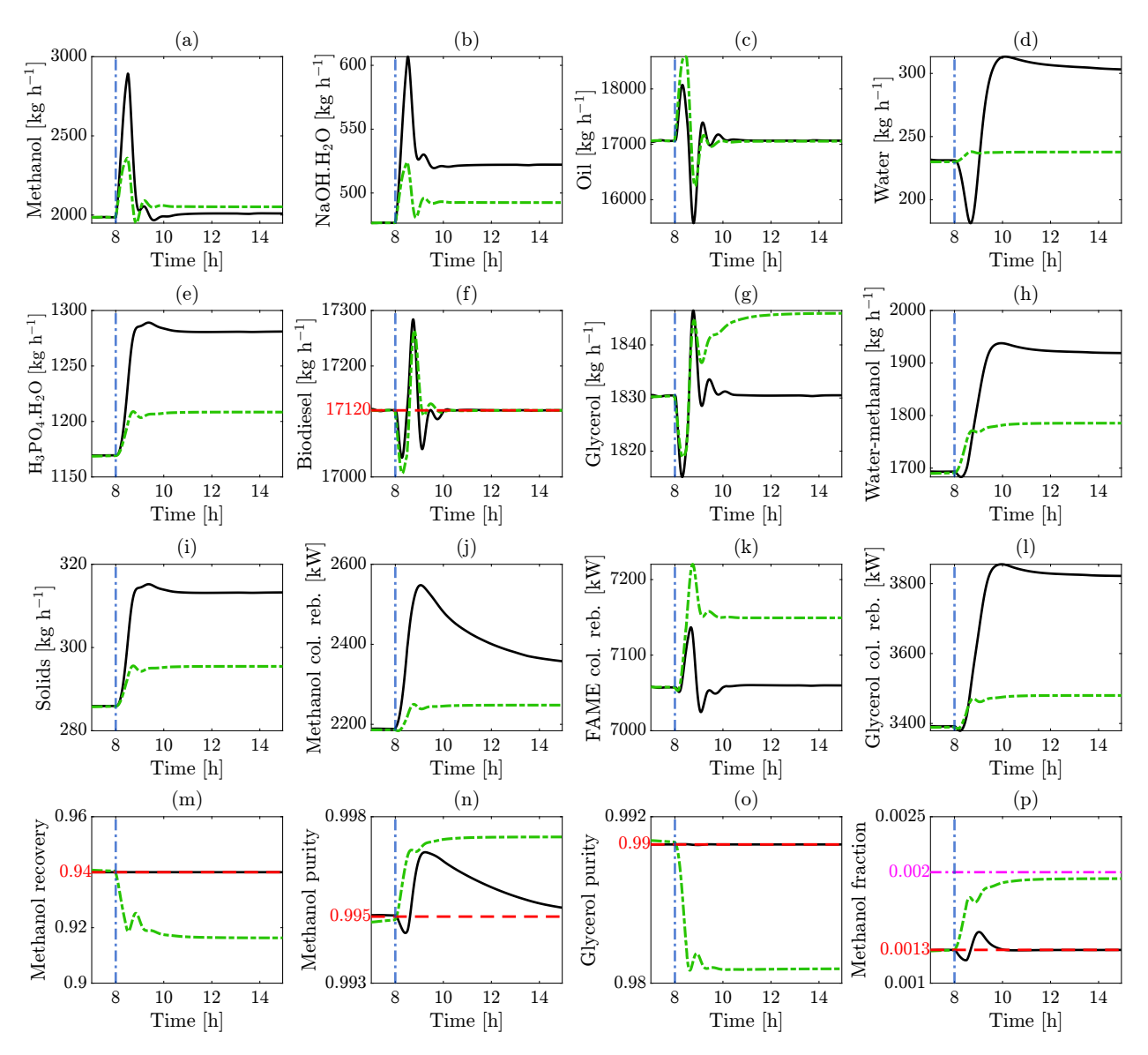


Figure 6: The profiles for the scenario SD1 of 20% decrease in the forward reaction rate coefficients of the transesterification reactions as provided in Figure 2. The disturbance takes place at $t_{\rm k}=8$ h (vertical dashed-dotted-blue line). (a)–(e): feed mass flow rates. (f)–(i): product mass flow rates. (j)–(l): reboiler duties. (m): methanol recovery in the methanol column. (n): methanol mass fraction in the methanol column distillate. (o): glycerol mass fraction in the glycerol column bottom. (p): methanol mass fraction in the biodiesel product. The solid-black and dashed-dotted-green curves are for the results of PWC-A and PWC-B, respectively. The dashed-red and dashed-dotted-magenta lines are the setpoints and bounds, respectively.

of the fed water into the columns. As aforesaid, when more water enters the columns (cf. Figures 7b, 7d and 7e), the enthalpies of vaporization in the reboilers increase and thus their duties.

Since in the case of PWC-B higher amount of methanol is fed (Figure 7a), while having lower recoveries in the methanol column, a higher amount of methanol enters the wash column. The ratio controller RC|300 that manipulates the fed water flow rate (Figure 7d) follows the total amount of the input raffinate and not that of methanol only. Therefore, higher concentrations of methanol remain in the raffinate stream that enters the FAME column. As a result, the mass fraction of methanol in the final biodiesel product increases from the previous steady-state value and gets beyond the permitted bound, as shown in Figure 7p. Moreover, the ratio controller RC|600 could not bring the glycerol mass fraction to the desired purity in the produced glycerol product. Therefore, under this disturbance, the implemented PWC-B could not satisfy the quality constraints on the final products.

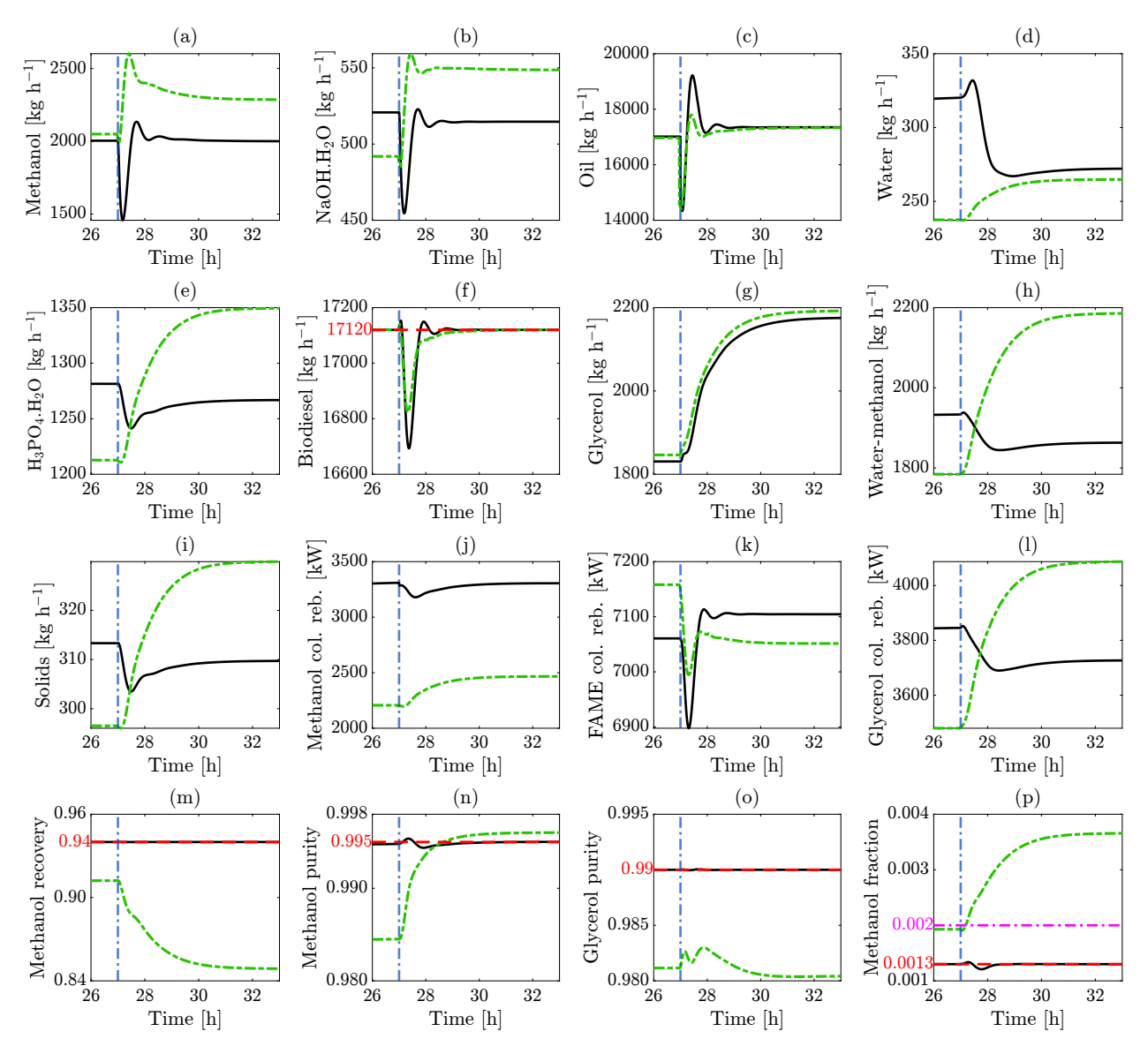


Figure 7: The profiles for the scenario SD6 of the change in the fed oil composition as provided in Figure 2. The disturbance takes place at $t_{\rm feed}=27$ h (vertical dashed-dotted-blue line). (a)–(e): feed mass flow rates. (f)–(i): product mass flow rates. (j)–(l): reboiler duties. (m): methanol recovery in the methanol column. (n): methanol mass fraction in the methanol column distillate. (o): glycerol mass fraction in the glycerol column bottom. (p): methanol mass fraction in the biodiesel product. The solid-black and dashed-dotted-green curves are for the results of PWC-A and PWC-B, respectively. The dashed-red and dashed-dotted-magenta lines are the setpoints and bounds, respectively.

6.2.4. Quantitative measures of dynamic performance

We present measures to quantitatively assess the dynamic performance of PWC-A and PWC-B. A suitable performance measure should capture essential process behavior, and be easily measurable and reliable. Based on Vasudevan and Rangaiah (2010)⁸⁸ and Kariwala and Rangaiah (2012),³ we use three performance criteria which are: (a) the accumulation-based settling time, which is the time required for the overall accumulation in process units to settle;³ (2) the integral of the overall accumulation;⁸⁹ and (3) the integral of the deviation from the production target.⁸⁸ Table 5 provide the results of the three criteria for both PWC-A and PWC-B.

Table 5: Quantitative performance assessment of the developed PWC structures. The results for PWC-B are shown in parentheses.

| Scenarios | Accumulation-based settling time [h] | Integral of the overall accumulation [kmol] | Integral of the deviation from the production target [kg] |
|-----------|--------------------------------------|---|--|
| ST1 | 5.4 (5.4) | 188 (188) | 1079 (961) |
| SD1 | 2.8(2.8) | 204 (194) | 101 (95) |
| SD2 | 0 (0) | 188 (188) | 0 (0) |
| SD3 | 1.6 (1.6) | 189 (187.6) | 32 (37) |
| SD4 | 2 (2) | 188 (188) | 268 (283) |
| SD5 | 0 (0) | 188 (188) | 0 (0) |
| SD6 | 3.5(4) | 190 (210) | 191 (158) |

The provided values in Table 5 are for applying the disturbances solely and not consecutively as shown in Figure 2. The settling times for both PWC structures are similar for all disturbances except for SD6. It is higher for PWC-B. This can be explained by the feed and product flow rate profiles in Figure 7, in particular, the methanol feed flow rate. As aforementioned, SD2 and SD5 have no effects on the process dynamics. This explains their zero values of settling times and deviations from the production target. For both PWC structures, the production rate follows its target well (cf. Figures 5f, 6f, and 7f), as the integral of the deviation from the production target for all scenarios is significantly small compared to the production target. The highest value is for PWC-A for ST1 and is less than 1.2 % of the total nominal production amount over 5.4 h.

Recall that due to the interconnected unit operations with plantwide control loops and recycle streams from the methanol and FAME columns, the analysis of the dynamic behavior of process variables and control loops should be carried out in a plantwide context. Overall, the applied PWC-A assumes that the control structure has an information-rich measurement configuration, which makes it highly suitable for the plant and yields satisfactory performance. The PWC-B, which relies solely on conventional measurement, is capable of satisfactorily handling scenarios involving changes in biodiesel production setpoint. Its control loops exhibit similar behavior to those of PWC-A. However, for the second and last disturbance scenarios, the control structure fails to meet the necessary standards for the final product quality, particularly the maximum allowable methanol concentration in the biodiesel product, due to a lack of measurements. These two disturbances involve changes in the reaction rates and fed oil composition that directly affect the quality of the products produced. As a result, by utilizing the IFSH method for two measurement-availability scenarios, we can provide insights into the need for process analytics. Specifically, the importance of inline concentration measurements for process control could be demonstrated, which is motivated by recent advancements in process analytics and spectrometry. Conversely, in situations where few conventional measurements are available, the importance of developing dynamic models for use in model-based control and estimation applications was shown. This underscores the significance and relevance of our developed model and implemented PWC structures for benchmark purposes.

While having information-rich measurements would be desirable, this does not correspond to current industrial practice. Thus, alternative control techniques should be considered to overcome the aforementioned limitations in the absence of information-rich measurements. Modern concepts, such as hierarchical control strategies including model predictive control, state estimation, and soft sensors, are promising solutions. Herein, the system observability needs to be considered. Notably, dynamic models, such as our proposal, need to be utilized for such model-based control and estimation methods.

7. Conclusion

We develop a detailed mechanistic dynamic model with rigorous thermodynamics for a biodiesel production plant via the production route of homogeneous alkali-catalyzed transesterification of vegetable oil. The model is implemented in Modelica with modular and hierarchical building blocks and provided open-source. Because we decouple the equations of the model components, the model could be adapted for other processes and used for modeling and simulating chemical processes in general. Therefore, using other production-route alternatives like homogeneous acidic or heterogeneous, utilizing other vegetable oils, or adding the oil (waste cooking oil) pretreatment process should be straightforward.

Moreover, we build a similar process in Aspen Plus and show that its steady-state results are very close to that of the proposed Modelica dynamic Model. Commercial tools like Aspen Plus are often used in academia and industry for process modeling and simulation. However, their model equations are not accessible and editable. In contrast, our proposed dynamic model is open-source and modular with full control on model equations. Such models are needed for optimization and model-based studies as well as for benchmark purposes. Notably, the proposed model shares many features with general chemical processes, particularly, it has the reaction, separation, and recycle parts. This underlines its generic value and significance as an open-source model.

We develop and implement two PWC structures based on the IFSH methodology. The PWC structures are based on decentralized PID controllers. The first control structure is based on the assumption of having information-rich measurement configurations (quality measurements), motivated by recent advances in process analytical technology and spectroscopy. In the other structure, we consider that only conventional measurements are available. Thus a structure that more matches current industrial practice. We study the dynamic behavior of the plant and conduct comparisons between the two applied PWC structures by simulating it under several plantwide disturbances and production rate setpoint changes. The plantwide analysis of the process variable profiles and control loops shows how the process units are interconnected with recycle streams and control loops and their interrelated dynamic behavior. The first PWC structure is adequate for the plant and performs satisfactorily in terms of setpoint tracking and disturbance rejection. The second PWC structure fails to satisfy product quality constraints at all times and thus cannot achieve the PWC objectives of the plant. Its behavior deviates from the first PWC structure, especially for the drop in the forward reaction rate coefficients and change in feed composition disturbances. This performance comparison between the two PWC structures and the limitations of the one that is based on conventional measurements motivate the importance of more advanced control strategies. Model-based control and estimation techniques in hierarchical control structures can be potential solutions to overcome the aforementioned limitations of conventional decentralized PID controllers. This reflects the importance of developing dynamic models of biodiesel production processes that can be utilized for such model-based control.

The developed model and PWC frameworks may be used to support the scaleup of biodiesel production processes, for instance, in terms of sizing of equipment, and identification of potential bottlenecks (e.g., availability of reactants, reactor residence time, catalyst alternatives, and important recycle streams). The model can also be employed as a digital twin for biodiesel production plants as well as for model-based experimental design applications. However, experimental validation of the model is still needed and can be conducted as future work.

We designed the process and fixed some setpoint values based on reported operating parameters in the literature. Some of those reportedly optimal values were determined for single process units (e.g., transesterifier) and not in a plantwide context. It is thus suggested to apply numerical optimization for the synthesis and design of sustainable biodiesel processes in a plantwide context. Optimal control problems can be formed, for instance, to minimize methanol usage, energy consumption, wash water usage, or waste streams. Moreover, (economic nonlinear) model predictive control methods may be employed to operate the process flexibly based on economical objectives while satisfying all operational and quality constraints. Mass integration synthesis along with heat integration can also be conducted for process optimization. Furthermore, the process model may be extended with respect to the characterization of the oil feed as well as the upstream processing like the pretreatment of waste cooking oil or preparation of algae oil.

8. Data availability

The Modelica model of the biodiesel production plant with its plantwide control structures is available under permalink.avt.rwth-aachen.de/?id=135903.

9. Supporting information

Detailed documentation of model equations for unit operations and thermodynamic calculations. Process flowsheet of the considered biodiesel production plant with controllers for implementing the PWC structure having conventional measurement configurations available (PWC-B). Tables with comparison of process steady-state simulation results: Aspen Plus model vs our proposed Modelica model. Additional results from the process dynamic simulations for both PWC-A and PWC-B structures, including all disturbances. This information is available free of charge via the Internet at http://pubs.acs.org/.

10. Acknowledgments

The authors gratefully acknowledge the financial support of the Kopernikus project SynErgie by the German Federal Ministry of Education and Research (BMBF) and the project supervision by the project management organization Projektträger Jülich (PtJ).

References

- (1) Scholl, K. W., Sorenson, S. C., Eds. Combustion of Soybean Oil Methyl Ester in a Direct Injection Diesel Engine, SAE International: 1993.
- (2) Wagner, L. E.; Clark, S. J.; Schrock, M. D. Effects of soybean oil esters on the performance, lubricating oil, and water of diesel engines; Society of Automotive Engineers, Inc., Warrendale, PA: United States, 1984.
- (3) Kariwala, V.; Rangaiah, G. P. *Plantwide Control: Recent Developments and Applications*; John Wiley & Sons Ltd: United Kingdom, 2012.
- (4) Okoye, P. U.; Longoria, A.; Sebastian, P. J.; Wang, S.; Li, S.; Hameed, B. H. A review on recent trends in reactor systems and azeotrope separation strategies for catalytic conversion of biodieselderived glycerol. *Science of The Total Environment* 2020, 719, 134595.
- (5) Demirbas, A. Biodiesel from vegetable oils via transesterification in supercritical methanol. *Energy Conversion and Management* **2002**, *43*, 2349–2356.
- (6) Maheshwari, P.; Haider, M. B.; Yusuf, M.; Klemes, J. J.; Bokhari, A.; Beg, M.; Al-Othman, A.; Kumar, R.; Jaiswal, A. K. A review on latest trends in cleaner biodiesel production: Role of feedstock, production methods, and catalysts. *Journal of Cleaner Production* 2022, 355, 131588.
- (7) Shahid, E.; Jamal, Y. A review of biodiesel as vehicular fuel. Renewable and Sustainable Energy Reviews 2008, 12, 2484–2494.
- (8) Martín, M.; Grossmann, I. E. Simultaneous Optimization and Heat Integration for Biodiesel Production from Cooking Oil and Algae. Industrial & Engineering Chemistry Research 2012, 51, 7998–8014.
- (9) Tayari, S.; Abedi, R.; Rahi, A. Comparative assessment of engine performance and emissions fueled with three different biodiesel generations. *Renewable Energy* **2020**, *147*, 1058–1069.
- (10) Zhang, Y.; Dubé, M. A.; McLean, D. D.; Kates, M. Biodiesel production from waste cooking oil: 1. Process design and technological assessment. *Bioresource Technology* **2003**, *89*, 1–16.
- (11) Nazir, N.; Ramli, N.; Mangunwidjaja, D.; Hambali, E.; Setyaningsih, D.; Yuliani, S.; Yarmo, M. A.; Salimon, J. Extraction, transesterification and process control in biodiesel production from Jatropha curcas. *European Journal of Lipid Science and Technology* **2009**, *111*, 1185–1200.
- (12) Freedman, B.; Butterfield, R. O.; Pryde, E. H. Transesterification kinetics of soybean oil 1. *Journal of the American Oil Chemists' Society* **1986**, *63*, 1375–1380.
- (13) Abbaszaadeh, A.; Ghobadian, B.; Omidkhah, M. R.; Najafi, G. Current biodiesel production technologies: A comparative review. *Energy Conversion and Management* **2012**, *63*, 138–148.
- (14) Vicente, G.; Martinez, M.; Aracil, J. Integrated biodiesel production: a comparison of different homogeneous catalysts systems. *Bioresource Technology* **2004**, *92*, 297–305.
- (15) Fukuda, H.; Kondo, A.; Noda, H. Biodiesel fuel production by transesterification of oils. *Journal of Bioscience and Bioengineering* **2001**, *92*, 405–416.
- (16) Mandari, V.; Devarai, S. K. Biodiesel Production Using Homogeneous, Heterogeneous, and Enzyme Catalysts via Transesterification and Esterification Reactions: a Critical Review. *BioEnergy Research* **2022**, *15*, 935–961.
- (17) Mohiddin, M. N. B.; Tan, Y. H.; Seow, Y. X.; Kansedo, J.; Mubarak, N. M.; Abdullah, M. O.; Chan, Y. S.; Khalid, M. Evaluation on feedstock, technologies, catalyst and reactor for sustainable biodiesel production: A review. *Journal of Industrial and Engineering Chemistry* 2021, 98, 60–81.
- (18) Salvi, B. L.; Panwar, N. L. Biodiesel resources and production technologies A review. *Renewable and Sustainable Energy Reviews* **2012**, *16*, 3680–3689.

- (19) Santori, G.; Di Nicola, G.; Moglie, M.; Polonara, F. A review analyzing the industrial biodiesel production practice starting from vegetable oil refining. *Applied Energy* **2012**, *92*, 109–132.
- (20) Enweremadu, C. C.; Mbarawa, M. M. Technical aspects of production and analysis of biodiesel from used cooking oil—A review. *Renewable and Sustainable Energy Reviews* **2009**, *13*, 2205–2224.
- (21) Haas, M. J.; McAloon, A. J.; Yee, W. C.; Foglia, T. A. A process model to estimate biodiesel production costs. *Bioresource Technology* **2006**, *97*, 671–678.
- (22) West, A. H.; Posarac, D.; Ellis, N. Assessment of four biodiesel production processes using HYSYS.Plant. *Bioresource Technology* **2008**, *99*, 6587–6601.
- (23) Apostolakou, A. A.; Kookos, I. K.; Marazioti, C.; Angelopoulos, K. C. Techno-economic analysis of a biodiesel production process from vegetable oils. *Fuel Processing Technology* **2009**, *90*, 1023–1031.
- (24) Myint, L. L.; El-Halwagi, M. M. Process analysis and optimization of biodiesel production from soybean oil. *Clean Technologies and Environmental Policy* **2009**, *11*, 263–276.
- (25) Santana, G.; Martins, P. F.; de Lima da Silva, N.; Batistella, C. B.; Maciel Filho, R.; Wolf Maciel, M. R. Simulation and cost estimate for biodiesel production using castor oil. *Chemical Engineering Research and Design* 2010, 88, 626–632.
- (26) Lee, S.; Posarac, D.; Ellis, N. Process simulation and economic analysis of biodiesel production processes using fresh and waste vegetable oil and supercritical methanol. *Chemical Engineering Research and Design* 2011, 89, 2626–2642.
- (27) Zavarukhin, S. G.; Yakovlev, V. A.; Parmon, V. N.; Sister, V. G.; Ivannikova, E. M.; Eliseeva, O. A. Development of a process for refining rape seed oil into biodiesel and high-cetane components of diesel fuel. *Chemistry and Technology of Fuels and Oils* **2010**, *46*, 1–8.
- (28) Noureddini, H.; Zhu, D. Kinetics of transesterification of soybean oil. *Journal of the American Oil Chemists' Society* **1997**, *74*, 1457–1463.
- (29) Sharma, Y. C.; Singh, B.; Korstad, J. Latest developments on application of heterogenous basic catalysts for an efficient and eco friendly synthesis of biodiesel: A review. Fuel **2011**, 90, 1309–1324.
- (30) Kusdiana, D.; Saka, S. Kinetics of transesterification in rapeseed oil to biodiesel fuel as treated in supercritical methanol. *Fuel* **2001**, *80*, 693–698.
- (31) Vicente, G.; Martínez, M.; Aracil, J.; Esteban, A. Kinetics of Sunflower Oil Methanolysis. *Industrial & Engineering Chemistry Research* **2005**, 44, 5447–5454.
- (32) Wali, W. A.; Al-Shamma'a, A. I.; Hassan, K. H.; Cullen, J. D. Online genetic-ANFIS temperature control for advanced microwave biodiesel reactor. *Journal of Process Control* **2012**, *22*, 1256–1272.
- (33) Bildea, C. S.; Kiss, A. A. Dynamics and control of a biodiesel process by reactive absorption. *Chemical Engineering Research and Design* **2011**, *89*, 187–196.
- (34) Shen, Y. H.; Cheng, J. K.; Ward, J. D.; Yu, C. C. Design and control of biodiesel production processes with phase split and recycle in the reactor system. *Journal of the Taiwan Institute of Chemical Engineers* **2011**, *42*, 741–750.
- (35) da Silva, B. F.; Schmitz, J. E.; Franco, I. C.; da Silva, F. V. Plantwide control systems design and evaluation applied to biodiesel production. *Biofuels* **2021**, *12*, 1199–1207.
- (36) Bildea, C. S.; Kiss, A. A. Plantwide Control of a Biodiesel Process by Reactive Absorption In Computer Aided Chemical Engineering: 20 European Symposium on Computer Aided Process Engineering, Pierucci, S., Ferraris, G. B., Eds.; Elsevier: 2010; Vol. 28, pp 535–540.
- (37) Regalado-Méndez, A.; Romero, R.; Natividad, R.; Skogestad, S. In *Automation Control Theory Perspectives in Intelligent Systems*, ed. by Silhavy, R.; Senkerik, R.; Oplatkova, Z. K.; Silhavy, P.; Prokopova, Z., Springer International Publishing: Cham, 2016, pp 107–117.
- (38) Mjalli, F. S.; Hussain, M. A. Approximate Predictive versus Self-Tuning Adaptive Control Strategies of Biodiesel Reactors. *Industrial & Engineering Chemistry Research* **2009**, 48, 11034–11047.
- (39) Brásio, A. S.; Romanenko, A.; Fernandes, N. C.; Santos, L. O. First principle modeling and predictive control of a continuous biodiesel plant. *Journal of Process Control* **2016**, *47*, 11–21.
- (40) Benavides, P. T.; Diwekar, U. Optimal control of biodiesel production in a batch reactor: Part I: Deterministic control. Fuel 2012, 94, 211–217.
- (41) Benavides, P. T.; Diwekar, U. Optimal control of biodiesel production in a batch reactor: Part II: Stochastic control. Fuel 2012, 94, 218–226.
- (42) Benavides, P. T.; Diwekar, U. Studying various optimal control problems in biodiesel production in a batch reactor under uncertainty. Fuel **2013**, 103, 585–592.
- (43) Aspen Technology Inc Aspen Plus Leading Process Simulation Software AspenTech, 2022.
- (44) Aspen Technology Inc Aspen HYSYS Process Simulation Software AspenTech, 2022.
- (45) Chang, A.-F.; Liu, Y. A. Integrated Process Modeling and Product Design of Biodiesel Manufacturing. Industrial & Engineering Chemistry Research 2010, 49, 1197–1213.

- (46) Brásio, A. S.; Romanenko, A.; Leal, J.; Santos, L. O.; Fernandes, N. C. Nonlinear model predictive control of biodiesel production via transesterification of used vegetable oils. *Journal of Process Control* **2013**, *23*, 1471–1479.
- (47) Reza Talaghat, M.; Mokhtari, S.; Saadat, M. Modeling and optimization of biodiesel production from microalgae in a batch reactor. *Fuel* **2020**, *280*, 118578.
- (48) Aniya, V. K.; Muktham, R. K.; Alka, K.; Satyavathi, B. Modeling and simulation of batch kinetics of non-edible karanja oil for biodiesel production: A mass transfer study. *Fuel* **2015**, *161*, 137–145.
- (49) Cheng, L.-H.; Yen, S.-Y.; Chen, Z.-S.; Chen, J. Modeling and simulation of biodiesel production using a membrane reactor integrated with a prereactor. *Chemical Engineering Science* **2012**, *69*, 81–92.
- (50) Farobie, O.; Hasanah, N.; Matsumura, Y. Artificial Neural Network Modeling to Predict Biodiesel Production in Supercritical Methanol and Ethanol Using Spiral Reactor. *Procedia Environmental Sciences* 2015, 28, 214–223.
- (51) Renon, H.; Prausnitz, J. M. Local compositions in thermodynamic excess functions for liquid mixtures. AIChE Journal 1968, 14, 135–144.
- (52) Design Institute for Physical Property Data DIPPR Project 801, Full Version: Evaluated Standard Thermophysical Property Values; BYU DIPPR, Thermophysical Properties Laboratory: 2010.
- (53) Fritzson, P. Principles of Object-Oriented Modeling and Simulation with Modelica 3.3: A Cyber-Physical Approach, 2nd Edition; Wiley IEEE Press: Piscataway, NJ 08854, 2015.
- (54) Esmonde-White, K. A.; Cuellar, M.; Uerpmann, C.; Lenain, B.; Lewis, I. R. Raman spectroscopy as a process analytical technology for pharmaceutical manufacturing and bioprocessing. *Analytical and Bioanalytical Chemistry* **2017**, 409, 637–649.
- (55) Harms, Z. D.; Shi, Z.; Kulkarni, R. A.; Myers, D. P. Characterization of Near-Infrared and Raman Spectroscopy for In-Line Monitoring of a Low-Drug Load Formulation in a Continuous Manufacturing Process. Analytical Chemistry 2019, 91, 8045–8053.
- (56) Downs, J. J.; Skogestad, S. An industrial and academic perspective on plantwide control. *Annual Reviews in Control* **2011**, *35*, 99–110.
- (57) Luyben, W. L.; Tyréus, B. D.; Luyben, M. L. *Plantwide Process Control*; McGraw-Hill: New York, United States, 1998.
- (58) Skogestad, S. Control structure design for complete chemical plants. Computers & Chemical Engineering 2004, 28, 219–234.
- (59) De Araújo, A. C.; Govatsmark, M.; Skogestad, S. Application of plantwide control to the HDA process. I steady-state optimization and self-optimizing control. *Control Engineering Practice* **2007**, *15*, 1222–1237
- (60) De Araújo, A. C. B.; Hori, E. S.; Skogestad, S. Application of Plantwide Control to the HDA Process. II Regulatory Control. *Industrial & Engineering Chemistry Research* **2007**, *46*, 5159–5174.
- (61) Murthy Konda, N. V. S. N.; Rangaiah, G. P.; Krishnaswamy, P. R. Plantwide Control of Industrial Processes: An Integrated Framework of Simulation and Heuristics. *Industrial & Engineering Chemistry Research* 2005, 44, 8300–8313.
- (62) Narváez, P. C.; Rincón, S. M.; Sánchez, F. J. Kinetics of Palm Oil Methanolysis. Journal of the American Oil Chemists' Society 2007, 84, 971–977.
- (63) Yancy-Caballero, D. M.; Guirardello, R. Modeling and parameters fitting of chemical and phase equilibria in reactive systems for biodiesel production. *Biomass and Bioenergy* **2015**, *81*, 544–555.
- (64) Albuquerque, A. A.; Ng, F. T.; Danielski, L.; Stragevitch, L. Phase equilibrium modeling in biodiesel production by reactive distillation. *Fuel* **2020**, *271*, 117688.
- (65) Salehi, A.; Karbassi, A.; Ghobadian, B.; Ghasemi, A.; Doustgani, A. Simulation process of biodiesel production plant. *Environmental Progress & Sustainable Energy* **2019**, *38*, e13264.
- (66) Engerer, J. D.; Jackson, G. R.; Paul, R.; Fisher, T. S. In Volume 6B: Energy, American Society of Mechanical Engineers: 11152013.
- (67) British Standards Institution Automotive fuels Fatty acid methyl esters (FAME) for diesel engines Requirements and test methods: EN 14214:2008+A1:2009, 2010.
- (68) German Union for the Promotion of Oil and Protein Plants Annual Report 2020/2021: Biodiesel production capacities in Germany in 2020, 2020.
- (69) Manosak, R.; Limpattayanate, S.; Hunsom, M. Sequential-refining of crude glycerol derived from waste used-oil methyl ester plant via a combined process of chemical and adsorption. *Fuel Processing Technology* **2011**, *92*, 92–99.
- (70) Ciriminna, R.; Della Pina, C.; Rossi, M.; Pagliaro, M. Understanding the glycerol market. *European Journal of Lipid Science and Technology* **2014**, *116*, 1432–1439.

- (71) Glisic, S. B.; Orlović, A. M. Review of biodiesel synthesis from waste oil under elevated pressure and temperature: Phase equilibrium, reaction kinetics, process design and techno-economic study. *Renewable and Sustainable Energy Reviews* **2014**, *31*, 708–725.
- (72) Hagenmeyer, V.; Nohr, M. Flatness-Based Two-Degree-of-Freedom Control of Industrial Semi-Batch Reactors In *Control and Observer Design for Nonlinear Finite and Infinite Dimensional Systems*, Meurer, T., Graichen, K., Gilles, E. D., Eds.; Springer Berlin Heidelberg: Berlin, Heidelberg, 2005, pp 315–332.
- (73) Control and Observer Design for Nonlinear Finite and Infinite Dimensional Systems; Meurer, T., Graichen, K., Gilles, E. D., Eds.; Springer Berlin Heidelberg: Berlin, Heidelberg, 2005.
- (74) Raghunathan, A. U.; Soledad Diaz, M.; Biegler, L. T. An MPEC formulation for dynamic optimization of distillation operations. *Computers & Chemical Engineering* **2004**, *28*, 2037–2052.
- (75) Caspari, A.; Offermanns, C.; Schäfer, P.; Mhamdi, A.; Mitsos, A. A flexible air separation process: 1. Design and steady–state optimizations. *AIChE Journal* **2019**, *65*, 467.
- (76) Rackett, H. G. Equation of state for saturated liquids. *Journal of Chemical & Engineering Data* **1970**, 15, 514–517.
- (77) Poling, B. E.; Prausnitz, J. M.; O'Connell, J. P. *The properties of gases and liquids*, 5th ed.; McGraw-Hill: New York, 2001.
- (78) Aspen Technology Aspen Physical Property System: Physical property methods and models, Burlington, MA 01803-5501, USA, 2013.
- (79) Yu-Wu, Q. M.; Weiss-Hortala, E.; Barna, R.; Boucard, H.; Bulza, S. Glycerol and bioglycerol conversion in supercritical water for hydrogen production. *Environmental Technology* **2012**, *33*, 2245–2255
- (80) Jaegers, N. R.; Hu, W.; Weber, T. J.; Hu, J. Z. Low-temperature († 200 °C) degradation of electronic nicotine delivery system liquids generates toxic aldehydes. *Scientific Reports* **2021**, *11*, 7800.
- (81) Sakdasri, W.; Ngamprasertsith, S.; Saengsuk, P.; Sawangkeaw, R. Supercritical reaction between methanol and glycerol: The effects of reaction products on biodiesel properties. *Energy Conversion and Management: X* **2021**, *12*, 100145.
- (82) Shin, H.-Y.; Lim, S.-M.; Bae, S.-Y.; Oh, S. C. Thermal decomposition and stability of fatty acid methyl esters in supercritical methanol. *Journal of Analytical and Applied Pyrolysis* **2011**, *92*, 332–338.
- (83) Zhu, Y. An Experimental Study on Thermal Stability of Biodiesel Fuel, Master Thesis, Syracuse University, 2012.
- (84) Murthy Konda, N. V. S. N.; Rangaiah, G. P.; Krishnaswamy, P. R. A simple and effective procedure for control degrees of freedom. *Chemical Engineering Science* 2006, 61, 1184–1194.
- (85) Luyben, W. L.; Tyreus, B. D.; Luyben, M. *Plantwide process control*; McGraw-Hill: New York, United States, 1999.
- (86) Dassault Systèmes Dymola Systems Engineering, 2022.
- (87) University of California Santa Barbara DASSL: Software Computational Science and Engineering Research Group, 2022.
- (88) Vasudevan, S.; Rangaiah, G. P. Criteria for Performance Assessment of Plantwide Control Systems. Industrial & Engineering Chemistry Research 2010, 49, 9209–9221.
- (89) Konda, N. V. S. N. M.; Rangaiah, G. P. Performance Assessment of Plantwide Control Systems of Industrial Processes. *Industrial & Engineering Chemistry Research* **2007**, *46*, 1220–1231.